Supply-demand analysis of anaerobic free-energy metabolism in *Saccharomyces cerevisiae*

Marthinus Kroukamp

Thesis presented in partial fulfilment of the requirements for the degree of Master of Science (Biochemistry) at the University of Stellenbosch

Supervisor: Prof JM Rohwer

Co-supervisor: Prof JL Snoep

December 2003

Declaration

I, the undersigned, declare that the work contained in this thesis is my own original work and has not previously in its entirety or in part been subjected to any university for a degree.

_____ 18/11/2003

Signature Date

Summary

Scientists and biochemical engineers alike are very interested in the control and regulation of free-energy metabolism in micro-organisms, whether the findings purely satisfy scientific curiosity or translate into the meeting of biotechnology company deadlines. We used a rather fundamental approach to investigate experimentally the control and regulation of yeast free-energy metabolism in anaerobic chemostat cultures using supply-demand analysis. This conceptually simple, quantitative framework, however, may lead to insight into the control properties of various metabolic pathways to be used in biotechnological applications.

Supply-demand analysis is based on the theoretical framework of metabolic control analysis (MCA). Sections (of arbitrary size) of a metabolic pathway are grouped together around a linking metabolite. Those steps that produce the intermediate are combined into the *supply* block while the reactions that remove/consume the intermediate are grouped together as the *demand*. The elasticity coefficients of the supply and demand blocks (with regard to the linking metabolite concentration) can be used to determine the flux and concentration control coefficients by using the traditional MCA summation and connectivity theorems. Supply and demand rate characteristics are a powerful visual approach to determine and display the control structure of the pathway under consideration and sets supply-demand analysis apart from traditional top-down analysis.

Our first tool of analysis was a structured kinetic model of yeast growing in

a chemostat, constructed by using methods developed in our research group for modelling systems with variable volumes. Independent perturbations of the linking metabolite concentration resulted in a control profile where the control resided mainly in the demand (flux control coefficient of 0.92), as a result of a large negative supply elasticity. This elasticity, however, varied greatly under different conditions, leading to increased flux control by the supply in some cases.

We extended our research to an experimental setup of *Saccharomyces cerevisiae* growing in a glucose-limited chemostat supplemented with yeast extract as a source of carbon intermediates. This allowed glucose to act solely as the free-energy source, as confirmed by balancing the glucose flux with the fluxes towards the fermentation products, ethanol and carbon dioxide. We obtained the *supply* rate characteristic by perturbing the ATP demand through the addition of benzoate, which uncouples the proton gradient across the cell membrane. The *demand* rate characteristic was obtained by perturbing the ATP supply through changes in the dilution rate and thus the residual glucose concentration in the fermentor. The concentrations of ATP and ADP were measured using a luciferase bioluminescence assay, while the fermentation products were measured with HPLC and CO_2 with an acoustic off-gas analyser. For our experimental conditions the flux-control of energy metabolism resided predominantly in the supply with respect to the linking metabolite [ATP]/[ADP] (chosen as an indication of the free-energy state of the cell), i.e. a flux control coefficient of 0.90. Further, the [ATP]/[ADP] was under strong homeostatic control, as evidenced by the low [ATP]/[ADP] control coefficients of $\pm$ 0.12.

We adjusted the structured kinetic model by varying strategic parameters, so that the results resembled the experimental observations more closely. However, the kinetics of our core model seem to be too simplistic to capture fully the extent of regulation displayed by the experimental system. The model did, however, reveal the regulatory importance of glucose transport into the cell. We conclude that the control and regulation of free energy metabolism in yeast strongly depend on the

culturing conditions and on the steady state being analysed.

Opsomming

Wetenskaplikes sowel as biochemiese ingenieurs is dikwels geïnteresseerd in die beheer en regulering van vry-energie metabolisme in mikro-organismes, hetsy die bevindinge suiwer wetenskaplike nuuskierigheid bevredig of die haalbaarheid van biotegnologie-maatskappy-mikpunte beteken. Ons het 'n redelik fundamentele benadering gevolg om die beheer en regulering van vry-energie metabolisme in gis eksperimenteel te bepaal in anaerobiese chemostaatkulture met behulp van aanbod-aanvraag analise. Dit is 'n konseptueel eenvoudige, kwantitatiewe raamwerk met die potensiaal om insig te gee in die beheereienskappe van verskeie metaboliese paaie wat nuttig kan wees in biotegnologiese toepassings.

Aanbod-aanvraag analise is gebaseer op die teoretiese onderbou van metaboliese kontrole-analise (MKA). Dele (van arbitrêre grootte) van 'n metaboliese pad word gegroepeer rondom 'n verbindingsmetaboliet. Die stappe wat die intermediaat produseer word gekombineer as die *aanbod* terwyl die reaksies wat die intermediaat verbruik, saamgegroepeer word as die *aanvraag*. Die elastisiteitskoëffisiënte van die aanbod en aanvraag blokke (met betrekking tot die verbindingsmetaboliet-konsentrasie) kan gebruik word om die fluksie en konsentrasie kontrolekoëffisiënte te bereken met behulp van die sommasie en konnektwiteit teoremas van MKA. Aanbod en aanvraag snelheidskenmerkgrafieke is 'n treffende visuele benadering om die kontroleprofiel van die betrokke metaboliese pad te bepaal en te vertoon. Hierdie kenmerk onderskei aanbod-aanvraag analise van bo-na-onder analise.

Die eerste deel van ons ondersoek het behels 'n gestruktureerde kinetiese model (van gis wat groei in 'n chemostaat) met behulp van metodes wat in ons groep ontwikkel is om sisteme met variërende volumes te modelleer. Onafhanklike perturbasies van die verbindingsmetaboliet konsentrasie het gelei tot 'n kontroleprofiel waar die kontrole hoofsaaklik in die aanvraag gesetel was (fluksie kontrolekoëffisiënt van 0.92), as gevolg van 'n groot negatiewe aanbod-elastisiteit. Hierdie elastisiteit kan egter grootliks varieer tydens verskillende kondisies, wat lei tot 'n toenemende fluksie-beheer deur die aanbod in sommige gevalle.

Ons het ons navorsing uitgebrei na 'n eksperimentele opstelling van *Saccharomyces cerevisiae* wat groei in 'n glukose-gelimiteerde chemostaat, aangevul met gisekstrak as 'n bron van koolstof-intermediate. Dit bring mee dat glukose slegs as energiebron dien; dit is wel bevestig deur balanse op te stel van die koolstoffluksie vanaf glukose na koolstofdioksied en etanol as die fermentasieprodukte. Die *aanbod* snelheidskenmerkgrafiek is gegenereer deur die aanvraag van ATP te manipuleer deur middel van toevoeging van bensoaat, wat die protongradiënt oor die selmembraan ontkoppel. Die snelheidskenmerkgrafiek vir die *aanvraag* is gegenereer deur die aanbod van ATP te manipuleer deur middel van 'n variasie in die verdunningstempo en sodoende die residuele glukose konsentrasie in die fermentor. Die konsentrasies van ATP en ADP is bepaal deur middel van 'n lusiferase bioluminessensie-essai, terwyl die fermentasieprodukte met 'n HPLC en CO_2 met 'n akoestiese aflaatgasanaliseerder gemeet is. Vir die betrokke eksperimentele toestande was die fluksie-kontrole van energiemetabolisme oorwegend in die aanbod met betrekking tot die verbindingsmetaboliet, [ATP]/[ADP] (gekies as aanduiding van die vrye-energiestatus van die sel), naamlik 'n fluksie kontrolekoëffisiënt van 0.90. Verder was die [ATP]/[ADP] onder sterk homeostatiese beheer soos duidelik blyk uit die lae [ATP]/[ADP] kontrolekoëffisiënte van $\pm$ 0.12.

Ons het die gestruktureerde kinetiese model aangepas deur strategiese parameters te verander om sodoende die eksperimentele gedrag te probeer naboots. Die kinetika van ons kernmodel blyk egter te simplisties te wees om die volle omvang

van die regulering van die eksperimentele sisteem te vertoon. Die model het egter die belang van glukose transport oor die selmembraan aan die lig gebring. Ons kom tot die gevolgtrekking dat die beheer en regulering van vrye-energie metabolisme in gis sterk afhang van die groeitoestande sowel as die spesifieke bestendige toestand wat ondersoek word.

For my wife and parents

Acknowledgements

I would like to thank:

Prof Johann Rohwer for creating a relaxed and stimulating atmosphere for research and learning and for all the support in the form of mentoring and encouragement.

Prof Jacky Snoep for the valuable advice and support while Johann was away on sabbatical.

Leandro Boonzaaier, Wilma van Biljon and Hannes Slabbert for prayers and encouragement when everything went slow.

Arrie Arends, a fearless lab manager running a smooth lab, Christie Malherbe for help with the HPLC and Coen van der Weijden for continuous technical support throughout the duration of the project.

The National Research Foundation for providing financial assistance during my studies.

Contents

1 General Introduction

The similarities between a living cell and a factory regarding their activities and organisation are quite striking [1]. The quest to find out more about a living cell therefore often follows the same route as analysts would do when auditing a factory. In the case of a factory, this investigation process can arbitrarily be divided into three phases depending on the level of information required. On the first level, it is important to know *what* the factory actually does, i.e. information about the raw material being transported to the factory and processed (in a number of intermediate steps) into the desired products. The second level of information involves *how* the process is accomplished, e.g. knowledge about all the contributing steps, including rates and mechanisms of the appropriate machinery and their interactions. The third level focuses on *why* processes in the factory happen the way they do. At this level, internal factors like choice of raw material, choice of product, rate of manufacture, factory layout and internal regulatory mechanisms are justified and explained in terms of the market/economy in which this factory operates. Indeed, the survival of the factory depends on the efficiency of the manufacturing process and the ability to adapt to fluctuations in a fickle market environment.

In each instance in the previous paragraph, the word "factory" could have been replaced with the concept "living cell" and still satisfy current scientific reasoning. In this paper we studied living cells and addressed the question of "why things happen". The whole scaffold upon which our theoretical framework was built, how-

ever, rested on information gathered by scientists who asked descriptive (what) and mechanistic (how) questions.

Cellular systems display very high degrees of internal organisation. Their survival efficiency strongly relies on their ability to respond rapidly and appropriately to changes in internal and external environments. These changes may include variable fluxes, amounts of products and availability of resources, and should all be handled with relative ease. This ability to adapt to changes requires a survival strategy where effective control and regulation procedures are of utmost importance. In accordance with the factory analogy, we can only start to understand the function of the regulatory properties once we consider the external environment in which the cell operates. The whole integrated cellular system needs to be investigated in the same way that the activities of a factory need to be understood in terms of the economy within which it operates [2]. Attempts to study parts of the whole in isolation and making inferences about the rest of the system will reveal the lack of depth of understanding of the system.

The theoretical framework we used as the basis of this study is therefore aptly termed "supply-demand" analysis. Within this framework, cellular regulatory properties can be reported in terms of the environment in which the cells operate, almost like a cellular economy [2]. We used the control and regulation of anaerobic free-energy metabolism in *Saccharomyces cerevisiae* as our model system.

In the following introductory sections we will give an overview of pertinent yeast physiology, the regulation of glycolytic flux as well as the history of metabolic supply-demand theory and its main features.

1.1 Anaerobic Yeast Physiology

Yeasts are chemoorganotrophic micro-organisms, which means they derive their chemical energy in the form of ATP from the breakdown of organic compounds. All known yeasts can catabolise sugars as energy or carbon sources [3]. The two

main metabolic routes for the sugars to act as energy sources, are fermentation and respiration. The occurrence of either of these routes of free-energy transduction (and even the morphology of yeast cells [4] and organelles [5]) strongly depends on the external growth conditions encountered by the yeast.

According to Pronk *et al.* [6] all yeast strains predominantly use the Embden-Meyerhof pathway for the conversion of hexose phosphates to pyruvate. Glycolysis[1], which describes the cytosolic enzyme-catalysed conversion of glucose to pyruvate, provides free energy in the form of ATP, precursor metabolites and reducing power for biosynthetic pathways in the form of NADH. Under anaerobic conditions the pyruvate is decarboxylated before a final reduction to ethanol (this final reduction step ensures the regeneration of NAD^+ for use in glycolysis and thus maintains a redox neutral pathway). This process where yeasts use organic substrates anaerobically as electron donor, electron acceptor and carbon source is called fermentation [7]. When intermediates of the glycolytic pathway are withdrawn as precursors for biosynthetic pathways, not all the NADH produced can be regenerated into NAD^+. An alternative way to maintain the redox balance is the formation of reduced by-products like glycerol. However, this pathway is accompanied by diminished ATP/glucose production because the precursor of glycerol, dihydroxyacetone phosphate, was destined for ATP generation in the lower part of the Embden-Meyerhof pathway [7].

Under conducive conditions (presence of oxygen and absence of repression) *S. cerevisiae* can respire the pyruvate (formed during glycolysis) in the mitochondrial matrix. Respiration depicts the process where pyruvate is decarboxylated to acetyl CoA which enters the tricarboxylic acid cycle and is oxidised to CO_2 with the concomitant production of reduced redox carriers NADH and $FADH_2$. These reduced redox carriers are reoxidised, with oxygen being reduced to water in the final step. The electron transfer takes place in successive steps along the inner

[1] In the rest of this paper the term glycolysis will be used as a synonym for the Embden-Meyerhof pathway as is the case in *Saccharomyces cerevisiae*.

mitochondrial membrane. As electrons pass through the electron transport chain, protons are taken up from the mitochondrial matrix and released in the intermembrane space creating an electrochemical potential across the inner membrane. Protons flow back into the mitochondrial matrix through an ATP-synthase enzyme which drives ATP production. This process is termed oxidative phosphorylation.

Among the almost 800 yeast species [8], *Saccharomyces cerevisiae* has dominated the scientific arena mostly for historical reasons. For thousands of years it has reportedly accompanied humans, who used its ability to produce ethanol and carbon dioxide from sugars. The use of *S. cerevisiae* in the brewing and baking industry remains to this day, but has since been expanded to heterologous protein production [9], the production of fuel ethanol [10] and glycerol [11], as well as being used as a model for the regulation of fermentative metabolism [12].

With varying external conditions *S. cerevisiae* can derive its energy either from respiration or fermentation, or both. In aerobic glucose limited continuous cultures at dilution rates below 0.3 h^{-1} [13, 14] all the glucose is completely respired to CO_2 (i.e. all the free-energy is derived from respiration). In the presence of oxygen when the glucose concentration exceeds a certain threshold, *S. cerevisiae* can also use alcoholic fermentation together with respiration as a source of ATP. This particular respirofermentative usage of glucose is termed the Crabtree effect (for review see [15]).

In aerobic glucose-limited continuous cultures, dilution rates higher than 0.38 h^{-1} led to respiration and alcohol fermentation occurring concurrently, similar to the Crabtree effect [13]. Postma *et. al.* [13] concluded that the onset of alcoholic fermentation was not due to limited respiratory capacity, but rather to the uncoupling effect of weak organic acids excreted in the growth medium. This proposal was confirmed when alcoholic fermentation already started at a dilution rate of 0.30 h^{-1} with the addition of propionate. The uncoupling effect of weak acids (acetate and propionate) on *anaerobic* growth was confirmed in experiments by Verduyn *et al.* [16]. The proposed mechanism of action is that undissociated acid diffuses across

the plasma membrane and dissociates in the more alkaline intracellular environment (pH ± 7.0) [15, 16, 17]. This drop in cytosolic pH is counteracted by the plasma membrane ATPase that pumps out the excess protons with the concomitant hydrolysis of ATP. Thus additional ATP has to be generated to compensate for the influx of acid. Benzoic acid later became the uncoupling weak acid of choice, as *S. cerevisiae* is not able to metabolise it [18]. The pH of the culture vessel plays an important role in the benzoate assimilation. The pK_a value of benzoic acid is 4.19 and the fraction of undissociated acid will increase with decreasing pH [16].

S. cerevisiae is one of the few yeasts able to grow under strictly anaerobic conditions because of a good fermentative capacity [19]. (We exploited this property in our experimental setup as explained in Chapter 3 on page 30). The specific growth rate is only approximately 25 % lower under anaerobic conditions than aerobic conditions [14]. Anaerobic growth is, however, sub-optimal in mineral media without the addition of both sterols and unsaturated fatty acids [20, 21] as these compounds cannot be synthesised in the absence of oxygen. Ergosterol (the preferred sterol synthesised by yeast) contributes to maintaining an appropriately fluid phospholipid membrane environment [22]. Under aerobic conditions, yeast cannot take substantial amounts of ergosterol from the growth medium (a phenomenon called aerobic sterol exclusion) but ergosterol uptake proceeds readily under anaerobic conditions [22].

It should be noted that despite the overall agreement in many metabolic and physiological phenomena displayed by different *S. cerevisiae* strains, it would be prudent not to generalise or extrapolate all findings without careful investigation [9, 14].

1.2 Regulation of glycolytic flux

All science is not driven by industrial applications, but *S. cerevisiae*'s usefulness to human kind has certainly impacted the directions taken in modern research. It is

understandable that knowledge of metabolic regulation is crucial to yeast biotechnology where manipulation and directed control of yeast metabolism is exploited to deliver the desired products (biomass, ethanol, excreted proteins).

The bakery industry aims for maximum biomass formation (obtained when yeast fully respires its substrate which leads to maximal ATP yield) during the production stage of bakers' yeast, but a high rate of alcoholic fermentation during the leavening stage of the dough [14]. The state of full respiration can be achieved by manipulating the sugar concentration in the medium or the growth rate. The alcoholic beverage industry and the fuel ethanol industry on the other hand are not too concerned with biomass formation, but rather the complete fermentation of the sugars to alcohol and CO_2 [23] (the secondary effect of the production of flavour compounds and glycerol in the wine industry aside [24]).

Traditionally two types of approaches have been followed in an attempt to steer or manipulate the metabolism of micro-organisms. The classical engineering approach tries to determine optimum process parameters like the proper sugar concentrations, growth rate, pH, temperature and the most appropriate strain. In contrast, the following paragraph will briefly mention some of the more fundamental approaches that tries to explain "why" yeasts display different modes of metabolism (especially regarding glycolytic flux) under differing conditions.

Yeast metabolism and its regulation have been described in terms of many frameworks over the years. Early scientists realised that different yeasts were able to grow *only* in the presence of oxygen, *only* in the absence of oxygen or in either the presence or absence of oxygen respectively (e.g. [25]). They (early scientists) realised that the mode of energy metabolism (fermentation or respiration or both) was dependent on external growth conditions like the availability of glucose and oxygen [7]. (Today we know, however, that parameters like dissolved CO_2 concentration [26] and growth factor requirements [27] play an equally important role). The yeasts that were able to grow in either the presence or absence of oxygen were termed facultative fermentative. Among the facultative fermentative yeasts, there

exists quite a diversity of regulatory phenomena of alcoholic fermentation. These regulatory phenomena were named after their discoverers, e.g. the 'Pasteur effect', the 'Crabtree effect' [12], the 'Kluyver effect' and the 'Custers effect', and represent regulatory mechanisms that affect the balance between respiration and fermentation [6]. *S. cerevisiae* is a facultative fermentative yeast (although not a classical example [7]) and therefore capable of displaying both the Pasteur effect (the suppression of fermentation by oxygen [7]) and the Crabtree effect, where fermentation and respiration co-exist as energy producing pathways under conditions of oxygen availability and glucose excess [13]. The Crabtree effect, for example, is explained in terms of proposed mechanisms like catabolite repression [28, 29] (when glucose or initial product of glucose metabolism represses the synthesis of various respiratory and gluconeogenic enzymes) or catabolite inactivation (the rapid disappearance of respiratory enzymes upon the addition of glucose) [12, 30] or limited respiratory capacity [31, 32] which leads to an overflow reaction at pyruvate as the starting metabolite for both fermentation and respiration [6, 32, 33]. In the following paragraphs some of the current reasoning regarding glycolytic regulation in yeast, as well as theoretical and experimental tools, will be discussed.

It should be noted that regulatory mechanisms are always subjected to the stoichiometric constraints of the system, e.g. the relative amount of ethanol and CO_2 formed from glucose, ethanol that exerts end product inhibition on growth [34], and the requirement of redox balancing that may contribute to slight variations in the partitioning of metabolite fluxes [35, 36, 37, 38].

Since the stoichiometry places a constraint on the maximal amount of ethanol produced from glucose, the only area left to manipulate is the *flux* of glucose to its products. Classical reasoning on how to achieve this is first to familiarise oneself with the system, and once the participating components have been identified, to remove bottlenecks and inhibitory steps. The relevant regulatory components in the ethanol producing "machinery" of yeast were identified as glucose uptake [39, 40, 41], glycolysis (conversion of glucose to pyruvate) and the reduction of

pyruvate to ethanol. In glycolysis, phosphofructokinase [42] was identified as a "pace maker" enzyme due to its allosteric properties, and to remove this bottleneck it was overexpressed singularly and in pairs together with other glycolytic enzymes in yeast. This overexpression, however, did not lead to an increase in glycolytic flux [43]. The reduced flux control of the regulatory enzyme during feedback inhibition on the inhibited step has been proven mathematically by Kacser and Burns [44] and emphasizes the fact that control is shared among the steps in a metabolic pathway [45]. Similar studies investigated glucose transport into the cell as the possible important step in regulating glycolytic flux [40, 46, 47] and found that indeed the transport step has substantial but not complete control.

Although ATP production may have been implied in glycolytic flux regulation in the studies mentioned in the previous paragraphs, it was not mentioned explicitly. The role of ATP as regulator of glycolytic flux is treated in the literature in two distinct ways. The first one is an experimental and direct approach, where a decrease in glycolytic flux was observed with increasing ATP concentration [48, 49]. These studies focused on possible activation or inhibitory effects of ATP concentration on the activity of glycolytic enzymes like phosphofructokinase, pyruvate kinase and hexokinase. In both these studies by Larsson *et al.*, it was stressed that ATP does not seem to be the sole regulator of glycolytic flux. The second and more indirect approach proposed theoretically that ATP "utilisation" was a likely candidate for the regulation of glycolytic flux [50, 51, 52]. Theoretical studies by Hofmeyr and Cornish-Bowden also showed that the more control ATP demand ("utilisation") has on the flux, the less control it has on determining the degree of homeostasis and the distance from equilibrium where homeostasis is maintained [53, 2, 54, 55]. These results can therefore explain the ability of yeast to display great variations in glycolytic flux while maintaining the concentrations of the internal metabolites at a constant level (homeostasis). (The increase of glycolytic flux with the addition of weak acids to the culture medium, is for example, the result of a greater ATP demand for maintenance purposes [18].) The concept of ATP utilisation as a regu-

lating factor in glycolysis led to the formalisation of *supply-demand analysis* [2]. In the next four sections we will briefly discuss the history of supply-demand analysis (built on the theory of metabolic control analysis) and the developments that led to its formulation.

1.2.1 Metabolic control analysis

Metabolic control analysis (MCA) is a theoretical framework with which metabolic regulation and control can be described quantitatively for steady-state systems, and was independently developed by Kacser and Burns [44, 56] and Heinrich and Rapoport [57]. In essence it is a sensitivity analysis that quantifies the dependence of system variables on system parameters. According to Hofmeyr and Cornish-Bowden [54], system parameters are those quantities (e.g. concentrations of enzyme and cofactors or external effectors such as inhibitors, activators and growth factors) through which the environment can affect the system and determine the steady-state values of the fluxes and the intermediate metabolite concentrations (the dependent variables of the system).

On a *global* level metabolic control analysis allows us to describe the fractional (or percentage) change in a steady-state variable (flux or metabolite concentration) in response to a one percent change in the activity of a step (e.g. an enzyme catalysed reaction) in the system with a *control coefficient*. Mathematically the control coefficient ($C^{y}_{v_i}$) is defined as:

$$C^{y}_{v_i} = \frac{(\partial \ln y_j / \partial \ln p)_{ss}}{(\partial \ln v_i / \partial \ln p)_{\text{step } i}} \tag{1.1}$$

where y is any variable of the system and v_i is the activity of the step and p is a parameter that affects the activity of step i only. The subscript ss indicates that the entire system relaxes to a new steady state after a change in p, and the subscript *step i* indicates that only the change in the local rate v_i of step i is considered at constant reactant, product and effector concentrations.

The *local* properties of an enzyme reaction are expressed with *elasticity coefficients*, $\varepsilon_{s_j}^{v_i}$, which quantify how the reaction rate of the enzyme varies with changing concentrations of metabolites s_j that interact directly with the enzyme (e.g., substrates, products or cofactors). The elasticity coefficients are defined in a similar way to the control coefficients:

$$\varepsilon_{s_j}^{v_i} = \frac{\partial v_i / v_i}{\partial s_j / s_j} = \left(\frac{\partial \ln v_i}{\partial \ln s_j} \right)_{s_k, s_l, \ldots} \tag{1.2}$$

where v_i is the net rate through reaction i and s_j the concentration of the interacting metabolite. The subscripts s_k, s_l, ... indicate that the other metabolites are kept constant at their prevailing steady state values.

The control and elasticity coefficients adhere to certain constraints and interrelationships termed the summation and connectivity theorems of metabolic control analysis [56]. The *summation* theorem for flux control coefficients states that the sum of all the control coefficients for a given flux J over all the n enzymes in the system sums to one:

$$\sum_{i=1}^{n} C_{v_i}^{J} = 1 \tag{1.3}$$

This theorem implies that no single enzyme step necessarily controls the flux but that control is shared among the contributing enzymes.

The *connectivity* theorem states that the elasticity coefficients responding to a metabolite concentration s, relate to the flux control coefficients in the following way:

$$\sum_{i=1}^{n} C_{v_i}^{J} \varepsilon_{s}^{v_i} = 0 \tag{1.4}$$

For concentration-control coefficients the summation theorem can be written as:

$$\sum_{i=1}^{n} C_{v_i}^{s_j} = 0 \tag{1.5}$$

The connectivity theorem for concentration control coefficients has different forms depending on whether the metabolite whose concentration is the subject of the control coefficient (say s_j), differs from the one used in the elasticities (say s_k),

$$\sum_{i=1}^{n} C_{v_i}^{s_j} \varepsilon_{s_k}^{v_i} = 0 \tag{1.6}$$

or whether it refers to the same concentration

$$\sum_{i=1}^{n} C_{v_i}^{s_j} \varepsilon_{s_j}^{v_i} = -1 \tag{1.7}$$

Traditionally, one of the goals Kacser and Burns [44] had in mind with metabolic control analysis was to: "marry theory to experiment and observation". Early experimenters, however, were limited to a great extent to *in vitro* systems because of the requirement to know the exact magnitude of perturbation in enzyme activity. Traditionally control coefficients were determined experimentally by manipulating enzyme activity by genetic means, titrating with purified enzyme or titrating with specific inhibitors (reviewed by Fell [58]). According to Cornish-Bowden [59] it was Kacser and Burns themselves [60] who made the first attempt to "liberate the field from the need to study purified enzymes" by proposing what is now known as the *double modulation method.* With the double modulation method all the elasticity coefficients in a linear pathway can be determined by measuring the changes in flux and concentrations of intermediates upon perturbations of the activities of the first and last enzymes in the pathway. The control coefficients can easily be calculated from these elasticities using the summation and connectivity theorems—even in *in vivo* systems.

1.2.2 Top-down analysis

A further development came when Brand and co-workers formalised "top-down" metabolic control analysis [61, 62, 63]. The name of this method arose to contrast it to the more classical "bottom-up" approach used in MCA up until then, where

each enzyme in a pathway was manipulated individually to determine the elasticity and control coefficients. Top-down control analysis groups parts of the pathway under consideration into blocks. The grouping is done in such a way that the blocks are connected via a single intermediate. The concentration of this intermediate metabolite can be perturbed in a number of independent ways. Measurement of the resulting connecting intermediate concentration and the steady-state flux will yield the elasticities of the blocks to the intermediate metabolite. From the elasticities, the control coefficients can be calculated by using the connectivity and summation theorems. Multiple application of the top-down approach to smaller blocks in the pathway will result in a progressively fuller picture of the control structure, yielding the same information as the bottom-up approach in the end. An advantage of the top-down approach is that it can be applied to metabolic pathways in organelles, whole homogenates, cells, organs or whole animals. Furthermore it aims to retain simplicity by choosing the grouping of blocks in such a way that the complexities introduced e.g. (by enzyme-enzyme interactions and channeling) are avoided.

Let us consider the scheme:

$$\mathrm{A} \xrightarrow{1} X \xrightarrow{2} \mathrm{B}$$

The two ends of a linear metabolic pathway are linked by an intermediate, X. The concentrations of A and B are assumed fixed. 1 and 2 are blocks of reactions that may contain enzymatic or non-enzymatic steps that are grouped together and should have a unique response to the linking metabolite, X . Furthermore, and importantly, there should be no interactions between the blocks other than through X. To determine the elasticity of the bottom end of the pathway to X experimentally, X can be changed by any way that excludes the bottom end of the pathway. The same principle applies to the top end of the pathway. One way how this can be done experimentally is with the double modulation method [60, 63]. To determine the elasticity of the bottom end of the pathway with respect to X, any step in the top end (rates or concentrations) can be varied. These changes will either increase

or decrease the concentration of X, and the resulting response of the bottom end to this independent change of X, can be studied. Again the same procedure can be applied to determine the elasticity of the top end of the pathway.

Top-down control analysis has since been expanded to accommodate systems with more than one common intermediate [64] and reaction blocks that "cross-talk" [65]. In systems with more than one common intermediate the top-down approach can be applied provided that the elasticity of a block to a particular intermediate is measured under conditions in which all other intermediates are held constant. Ainscow and Brand [65] discuss in their paper on cross-talking reaction blocks, that systems with feedback inhibition can be treated by introducing different system modulations, and fractional values should be ascribed to intermediates in blocks that share common elements.

1.2.3 Modular analysis

"Modular analysis" [66, 67, 68] is another development based on metabolic control analysis, to study the control and regulation of larger functional units of metabolism like glycolysis or oxidative phosphorylation. Kahn and Westerhoff [66] originally proposed the method to determine the control properties of systems that are not connected by mass flow. The decomposition of the system into appropriate modules, however, also allowed the treatment of highly complex situations *with* mass flow. In contrast to top-down control analysis, modular analysis can accommodate modules that have several throughput fluxes and are connected by more than one metabolite. In the case where two modules are connected via only one "independent bridging flux" (one intermediate), modular analysis and top-down analysis are essentially the same. Modular analysis has recently been generalised by Hofmeyr and Westerhoff [69].

Schuster *et al.* [67] describe how to decompose a metabolic network into appropriate modules and below we give the example of a simple unbranched reaction

scheme.

$$A \xrightarrow{1} X_1 \xrightarrow{2} X_2 \xrightarrow{3} X_3 \xrightarrow{4} B \tag{1.8}$$

If the modules in scheme 1.8 are chosen in the following way:

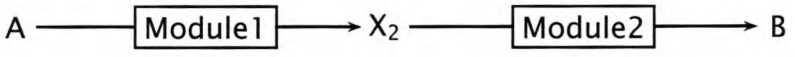

the treatment (determination of elasticity and control coefficients) of this simplified case would be the same as with top-down control analysis.

1.2.4 Supply-demand analysis

Supply-demand analysis is a refinement and extension of top-down metabolic control analysis. Hofmeyr and Cornish-Bowden [2] proposed this analysis based on their firm belief that metabolic control and regulation are "inextricably linked to function". This linking of understanding to function satisfies the "why" question mentioned in this chapter on page 1.

At this stage it may be useful to note that economists define *demand* as currency votes that people cast through an act of the will and *supply* as the quantity of a commodity that businesses willingly produce and sell [70]. Features of this economic model, like the law of downward sloping demand (people will buy more of a product if it is cheaper), therefore, cannot be extrapolated to the metabolic supply-demand analysis described below, because in cellular systems the supply and demand are governed by stoichiometric, thermodynamic and kinetic constraints.

Supply-demand analysis adheres to all the presciptions/requirements of top-down analysis described above and can be summarised with the following scheme:

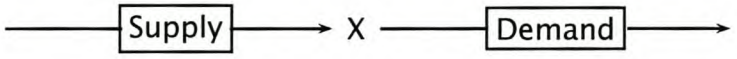

All the processes producing a linking metabolite, X, are blocked together into the *supply*, while all the consuming reactions are blocked together into the *demand*.

A very important feature of supply-demand analysis is the quantitative, visual representation of the behaviour of the supply and demand blocks with regard to the steady state concentration x [2], with graphs of combined rate characteristics [71]. The natural logarithms of the supply and demand rates are plotted against the natural logarithm of the steady state concentration of the linking metabolite. The intersection of these two rate characteristics represents the steady-state where the elasticities of the supply and demand, with respect to the same steady-state concentration of x, can be compared. The visual approach of using rate characteristics is a very useful tool in identifying *regions* where flux control or concentration control reside by just looking at the form of the supply or demand curves. This is possible because of the inherent requirement for multiple steady-states (at different linking metabolite concentrations[2]) to draw the rate characteristics. At any given point on the rate characteristic, the slope will thus give the elasticity for that *specific* linking metabolite concentration. This feature sets supply-demand analysis apart from traditional top-down analysis where claims can only be made about the specific steady-state point under consideration.

It follows from the definition of the elasticity coefficients that:

$$\varepsilon_x^{v_{\text{supply}}} = \frac{\partial \ln v_{\text{supply}}}{\partial \ln x} \tag{1.9}$$

$$\varepsilon_x^{v_{\text{demand}}} = \frac{\partial \ln v_{\text{demand}}}{\partial \ln x} \tag{1.10}$$

These elasticities can therefore be read from the graph as the slopes of the tangents to the intersection at the steady-state point. From the elasticities the flux

[2]The concept of making a series of changes of the same type but different sizes to determine elasticities was hinted at by Fell [58]. His aim, however, was not to draw rate characteristics but to construct initial slopes to overcome the restriction posed by MCA that only small perturbations can be used.

and concentration control coefficients can be calculated using the summation and connectivity theorems:

$$C^J_{\text{supply}} = \frac{\varepsilon_x^{\text{demand}}}{\varepsilon_x^{\text{demand}} - \varepsilon_x^{\text{supply}}} \tag{1.11}$$

$$C^J_{\text{demand}} = \frac{-\varepsilon_x^{\text{supply}}}{\varepsilon_x^{\text{demand}} - \varepsilon_x^{\text{supply}}} \tag{1.12}$$

$$C^x_{\text{supply}} = \frac{1}{\varepsilon_x^{\text{demand}} - \varepsilon_x^{\text{supply}}} \tag{1.13}$$

$$C^x_{\text{demand}} = \frac{-1}{\varepsilon_x^{\text{demand}} - \varepsilon_x^{\text{supply}}} \tag{1.14}$$

The informed reader will realise that equations 1.9 - 1.14 are classic metabolic control theory applied to a two step system with a linking metabolite (this will always be the case with supply-demand analysis). True to its origins, theoretical supply-demand analysis is also well suited for experimental verification.

1.3 Aim and outline of this thesis

The chronological events that led to the writing of this thesis might give some insight into the subsequent layout. Rohwer *et al.* [72] used a structured kinetic model to study the control and regulation of anaerobic free-energy metabolism of microorganisms growing in a chemostat within the framework of supply-demand analysis. Their modelling exploration pointed to possible improvements on their existing model which we mention and describe in Chapter 2.

In accordance with the philosophy of our research group we wanted to combine theory, modelling and experiment to aid in understanding rather than merely describing observations. For this reason we decided to investigate experimentally the control and regulation of anaerobic free-energy metabolism in *S. cerevisiae* using the theoretical framework of supply-demand analysis. The challenges of adapting the experimental setup to the requirements laid out by the theory are described in Chapter 3. The experimental supply and demand rate characteristics are presented in Chapter 4, as well as the results of the preparatory experimental con-

trols. Included in Chapter 4 is a brief discussion defending the rationale for the experimental approach.

A comprehensive general discussion about the project, results, (including further modelling results to incorporate the insights we gained from our experimental work) and future perspectives, appears in Chapter 5 and adds to (rather than repeats) the discussions in Chapter 4. Finally the experimental methods and calculations are described in Chapter 6.

2 Structured kinetic model of yeast energy metabolism

2.1 Introduction

Modelling is central to scientific investigation (the accumulation of knowledge about nature and the behaviour of the real world in terms of measurable entities and processes [73]). The necessity of models, as abstractions of real world situations, arises from the complexity displayed by real world systems because of either the very large number of contributing components and interactions or the occurrence of a "black box" that is inaccessible to experimental observation.

The purpose for experimental modelling can range from testing hypotheses rapidly, efficiently, and inexpensively to predicting the behaviour of the system of interest (see Massoud *et al.* [73] and Wiechert [74] for a more complete list of the purposes of experimental modelling). We primarily used our model to a) identify important parameters of the system, b) identify essentials of the system structure, and c) determine the overall system sensitivity to variation in parameters.

Extensive models of *S. cerevisiae* metabolism do exist in the literature. Duboc *et al.* [75] studied the dynamic (time-dependent) behaviour of the decoupling of anabolism and catabolism in continuous cultures. Lei *et al.* [76] modelled the overflow metabolism at the acetaldehyde and pyruvate branch points as a cause of the onset

of aerobic alcoholic fermentation. Hynne *et al.* [77] constructed a full-scale model of yeast glycolysis by fitting biochemical pathways to experimental substrate concentrations and dynamical properties where the kinetic parameters were lacking. Rizzi *et al.* [78] studied the dynamic behaviour of yeast glycolytic kinetics while Teusink *et al.* [79] compared kinetic characteristics of yeast glycolysis obtained *in vivo* with modelled behaviour (kinetic parameters obtained from *in vitro* properties of the constituent enzymes).

2.2 Model description, rate equations and ODEs

The aim of our modelling was to study the control and regulation of yeast energy supply and demand and we therefore used a simplified core model of yeast growing anaerobically in a chemostat. Our model is an adaptation of the one used by Rohwer *et al.* [72] who performed a modelling exploration of the control of free-energy metabolism in fermentative yeast (see Figure 2.1). Their model revealed the problems arising from using glucose as both carbon and energy source (interaction between the supply and demand blocks not confined to communication only via the linking metabolite as mentioned in Chapter 1 on page 12). The proposed solution was to supplement the medium with yeast extract to supply carbon intermediates. In this way glucose could act as the sole energy source and the energy *supply* could be separated from the energy *demand* as will be illustrated in the next section.

2.2.1 Communication only via linking metabolite

The framework of our study requires that the communication between the supply and demand blocks should only occur via the linking metabolite.

Figure 2.1 represents a core model of a microorganism growing in a chemostat on minimal media to demonstrate the problems associated with glucose as both carbon and energy source. It is clear that the substrate, S_i (glucose), is used in the supply (reaction $\boxed{2}$, Fig. 2.1) *and* the demand (reaction $\boxed{3}$, Fig. 2.1) of ATP and

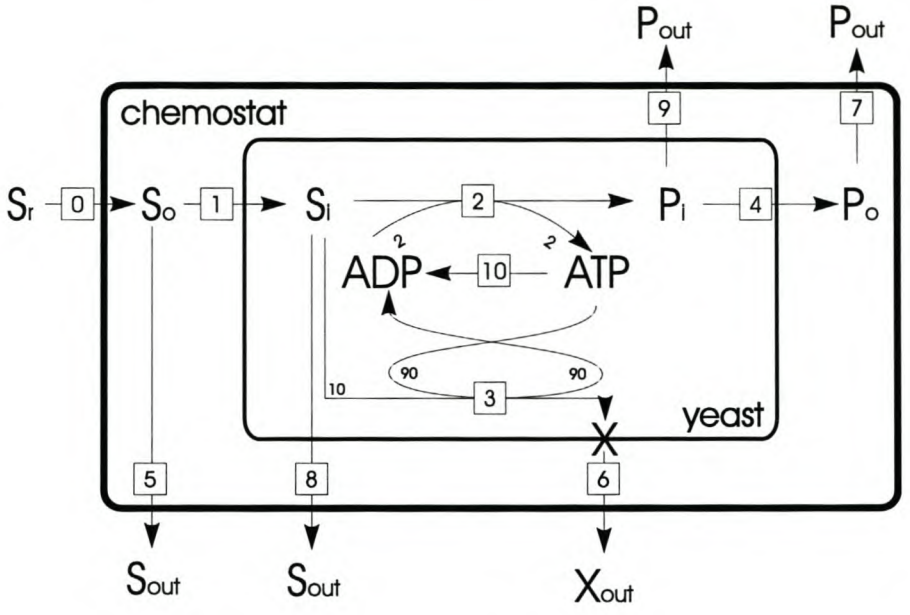

Fig. 2.1 Core model of yeast in a chemostat grown on minimal medium

violates the principle of communication via only the linking metabolite.

Supplementing the medium feed with yeast extract could possibly circumvent this problem as carbon building blocks are sequestered from the rich medium, as depicted schematically by Figure 2.2. In this way it should be possible to separate catabolism and anabolism and use glucose solely as energy source (reaction [2], Fig. 2.2) and yeast extract, R_i (reaction [3], Fig. 2.2) for biomass. At this stage the residual concentration of S_o in the chemostat is assumed to be constant throughout all these manipulations (the consequences and validity of this assumption will be discussed on page 46).

2.2.2 General model description

A graphical representation of the model we used is depicted in Figure 2.2. The conversion of glucose to ethanol was lumped together as one reaction and regarded as the only supply of energy in the form of ATP. The demand for ATP comprised of a non-growth component and a growth reaction that uses ATP and carbon inter-

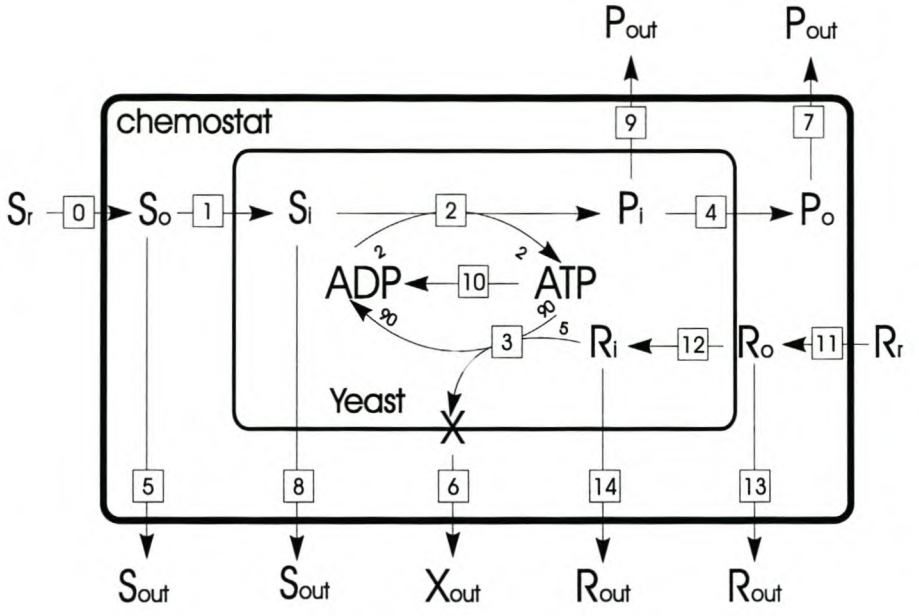

Fig. 2.2 Core model of yeast in a chemostat grown on rich media (minimal media supplemented with yeast extract). The stoichiometries are discussed on page 24.

mediates (provided by the yeast extract in the rich medium) to produce biomass. The transport steps across the cell membranes and ATP leak were modelled as reversible Michaelis-Menten reactions, while glycolysis and the growth reactions were modelled as reversible two-substrate two-product rate equations with independent binding sites [80]. Washout of metabolites internal and external to the yeast occurred in direct proportion to the dilution rate.

2.2.3 Rate equations and ODEs

We used mole amounts (rather than concentrations) in setting up the rate equations and ordinary differential equations (ODEs). This method, termed Model Formulation 1 (MF1) by Hofmeyr *et al.* (work in preparation), allows us to model compartmentalised systems with variable volumes. The models were coded in WinScamp [81] and Python/SciPy [82].

The notation in this section uses the convention of uppercase italic letters to

refer to *amounts* or *quantities* and lower case italics to refer to *concentrations*. We have tried to obtain values for the kinetic parameters of the rate equations from the literature where applicable. Because this is a core model, with many steps in a pathway often lumped into one reaction, we used estimates of the values for the kinetic parameters based on values of the same order of magnitude of the contributing reactions. (Reaction numbers in the text correspond to the reaction numbers in Figure 2.2). In the description of all the subsequent reactions the subscripts r, o and i refer to the medium feed (reservoir), chemostat compartment (outside) and the combined internal cellular compartment (inside) respectively. Furthermore, the substrate, S, refers to glucose and the product, P, to ethanol while R is the symbol used for the carbon intermediates (rich medium) added as yeast extract. The rate equations of reactions $\boxed{0}$ to $\boxed{14}$ (Figure 2.2) are given by equations 2.1–2.15.

Reaction $\boxed{0}$ depicts glucose feed into the chemostat with V_t as the total volume of the chemostat and s_r the molar concentration of glucose in the feed. D is the dilution rate with units of h^{-1}.

$$v_0 = D \cdot s_r \cdot V_t \tag{2.1}$$

The uptake of glucose (reaction $\boxed{1}$) was modelled as facilitated diffusion with the K_m of glucose uptake of 0.1 mM corresponding well with values obtained by Walsh *et al.* [83] for high affinity glucose uptake. All the transporters in the model were treated as symmetrical carriers. E_1 is the mole amount of carrier, and V_o and V_i are the volumes of chemostat and intracellular compartments.

$$v_1 = \frac{k_{cat1}E_1}{K_{m1(S_o)}}\left(\frac{\frac{S_o}{V_o} - \frac{S_i}{V_iK_{eq1}}}{1 + \frac{S_o}{V_oK_{m1(S_o)}} + \frac{S_i}{V_iK_{m1(S_i)}}}\right) \tag{2.2}$$

In reaction $\boxed{2}$ (glycolysis), "ADP" refers to the mole *fraction* of total amount (μmol) of adenylates that exists as ADP. Hence (1−ADP) is the mole fraction of ATP. This ensures that we can treat ATP and ADP as a moiety conserved cycle. α_T is the total

μmol adenylates per mg biomass and α_V is the internal volume of the cell in ml per mg biomass.

$$v_2 = \frac{k_{cat2}E_2}{K_{m2(S_i)}K_{m2(\mathrm{ADP})}} \left(\frac{\frac{S_i}{V_i}\mathrm{ADP}\frac{\alpha_T}{\alpha_V} - (1-\mathrm{ADP})\,\frac{\alpha_T}{\alpha_V}\frac{P_i}{V_iK_{eq2}}}{\left(1+\frac{S_i}{V_iK_{m2(S_i)}}+\frac{P_i}{V_iK_{m2(P_i)}}\right)\left(1+\frac{\mathrm{ADP}\cdot\alpha_T}{\alpha_VK_{m2(\mathrm{ADP})}}+\frac{(1-\mathrm{ADP})\cdot\alpha_T}{\alpha_VK_{m2(\mathrm{ATP})}}\right)} \right) \quad (2.3)$$

In the growth reaction (3), R, provides the carbon intermediates incorporated into biomass with the concomitant hydrolysis of ATP.

$$v_3 = \frac{k_{cat3}E_3}{K_{m3(R_i)}K_{m3(\mathrm{ATP})}} \left(\frac{\frac{R_i}{V_i}\,(1-\mathrm{ADP})\,\frac{\alpha_T}{\alpha_V} - \mathrm{ADP}\frac{\alpha_T}{\alpha_V}\frac{X}{V_oK_{eq3}}}{\left(1+\frac{R_i}{V_iK_{m3(R_i)}}\right)\left(1+\frac{(1-\mathrm{ADP})\cdot\alpha_T}{\alpha_VK_{m3(\mathrm{ATP})}}+\frac{\mathrm{ADP}\cdot\alpha_T}{\alpha_VK_{m3(\mathrm{ATP})}}\right)} \right) \quad (2.4)$$

Reaction 4 depicts the export of P by facilitated diffusion

$$v_4 = \frac{k_{cat4}E_4}{K_{m4(P_i)}} \left(\frac{\frac{P_i}{V_i} - \frac{P_o}{V_oK_{eq4}}}{1+\frac{P_i}{V_iK_{m4(P_i)}}+\frac{P_o}{V_oK_{m4(P_o)}}} \right) \quad (2.5)$$

Reactions 5 - 9 and 13 - 14 are the washout steps of metabolites and biomass from the chemostat. The internal metabolites are washed out as biomass exits the chemostat.

$$v_5 = D \cdot S_o \quad (2.6)$$

$$v_6 = D \cdot X \quad (2.7)$$

$$v_7 = D \cdot P_o \quad (2.8)$$

$$v_8 = D \cdot S_i \quad (2.9)$$

$$v_9 = D \cdot P_i \quad (2.10)$$

In reaction 10 the maintenance ATPase is modelled as a function of ATP and ADP using reversible Michaelis-Menten kinetics.

$$v_{10} = \frac{k_{cat10}E_{10}}{K_{m10(\mathrm{ATP})}} \left(\frac{(1-\mathrm{ADP})\,\frac{\alpha_T}{\alpha_V} - \mathrm{ADP}\frac{\alpha_T}{\alpha_VK_{eq10}}}{1+(1-\mathrm{ADP})\,\frac{\alpha_T}{\alpha_VK_{m10(\mathrm{ATP})}}+\mathrm{ADP}\frac{\alpha_T}{\alpha_VK_{m10(\mathrm{ADP})}}} \right) \quad (2.11)$$

In reaction [11] r_r is the concentration of yeast extract entering the chemostat.

$$v_{11} = D \cdot r_r \cdot V_t \tag{2.12}$$

Uptake of R is also assumed to occur through facilitated diffusion (reaction [12]).

$$v_{12} = \frac{k_{cat12}E_{12}}{K_{m12(R_o)}} \left(\frac{\frac{R_o}{V_o} - \frac{R_i}{V_i K_{eq12}}}{1 + \frac{R_o}{V_o K_{m12(R_o)}} + \frac{R_i}{V_i K_{m12(R_i)}}} \right) \tag{2.13}$$

$$v_{13} = D \cdot R_o \tag{2.14}$$

$$v_{14} = D \cdot R_i \tag{2.15}$$

Equations 2.16–2.23 are the set of ordinary differential equations that describe the time evolution of the system. The stoichiometric coefficient of 90 (in equation 2.23) for ATP hydrolysis was chosen to give an ATP yield of approximately 10.5 g dry mass/mol ATP [84]. R has the units of μmol and we assume an average M_r of 200 for the building blocks present in the yeast extract. This implies that 5 μmol of intermediates translates into 1 mg of biomass (hence the stoichiometric coefficient of 5 in equation 2.22).

$$\frac{dX}{dt} = v_3 - v_6 \tag{2.16}$$

$$\frac{dS_o}{dt} = v_0 - v_1 - v_5 \tag{2.17}$$

$$\frac{dP_o}{dt} = v_4 - v_7 \tag{2.18}$$

$$\frac{dR_o}{dt} = v_{11} - v_{12} - v_{13} \tag{2.19}$$

$$\frac{dS_i}{dt} = v_1 - v_2 - v_8 \tag{2.20}$$

$$\frac{dP_i}{dt} = v_2 - v_4 - v_9 \tag{2.21}$$

$$\frac{dR_i}{dt} = -5(v_3) + v_{12} - v_{14} \tag{2.22}$$

$$\frac{d(\mathrm{ADP})}{dt} = -2(v_2) + 90(v_3) + v_{10} \tag{2.23}$$

All the kinetic parameters of the reactions are summarised in Table 2.1, and Table 2.2 recalls the other model parameters and initial conditions.

Table 2.1 Kinetic parameters of the enzyme catalysed reactions

All k_{cat} values are in h^{-1} and K_m values in mM

Parameter	Value	Comment
Reaction 1: Glucose uptake (facilitated diffusion)		
k_{cat1}	4.0 x 10^6	
$K_{m1(S_o)}$	1	
$K_{m1(S_i)}$	1	symmetrical carrier
K_{eq1}	1	facilitated diffusion
Reaction 2: Glucose converted to product P with ATP production		
k_{cat2}	2.0 x 10^6	
$K_{m2(S_i)}$	0.01	"hexokinase" saturated with internal glucose
$K_{m2(P_i)}$	1	
$K_{m2(\mathrm{ADP})}$	0.1	
$K_{m2(\mathrm{ATP})}$	1	
K_{eq2}	1 x 10^5	
Reaction 3: ATP and yeast extract used in biomass formation		
k_{cat3}	1.1 x 10^4	
$K_{m3(R_i)}$	1	
$K_{m3(\mathrm{ATP})}$	0.1	
$K_{m3(\mathrm{ADP})}$	0.1	
K_{eq3}	1 x 10^5	
Reaction 4: Export of P by yeast (facilitated diffusion)		
k_{cat4}	6.0 x 10^6	
$K_{m4(P_i)}$	1	
$K_{m4(P_o)}$	1	symmetrical carrier
K_{eq4}	1	facilitated diffusion
Reaction 10: Maintenance ATPase		
k_{cat10}	2.7 x 10^4	
$K_{m10(\mathrm{ATP})}$	0.1	saturate with ATP and ADP (i.e. low K_m) to make dependent on ratio
$K_{m10(\mathrm{ADP})}$	0.1	
K_{eq10}	1 x 10^4	
Reaction 12: Uptake of carbon intermediates (facilitated diffusion)		
k_{cat12}	2.3 x 10^8	
$K_{m12(R_o)}$	1	
$K_{m12(R_i)}$	1	symmetrical carrier
K_{eq12}	1	facilitated diffusion

Table 2.2 Other parameters and initial conditions used in the model

	Value	Unit
Parameter		
α_T	0.025	total μmol adenylates/ml
α_V	0.005	internal volume (ml)/mg dry mass
s_r	50	mM
r_r	20	mM
D	0.2	h^{-1}
V_t	1000	ml
Initial condition		
X	1000	mg
S_o	200	μmol
S_i	0.5	μmol
P_o	50 000	μmol
P_i	100	μmol
R_o	15 000	μmol
R_i	0.9	μmol
ADP	0.5	mole fraction
ATP	0.5	mole fraction
V_o	995	ml
V_i	5	ml
P_{out}	0	
S_{out}	0	
X_{out}	0	
R_{out}	0	
α_{E1}	2.5×10^{-5}	μmol/mg dry mass
α_{E2}	2.5×10^{-5}	μmol/mg dry mass
α_{E3}	2.5×10^{-5}	μmol/mg dry mass
α_{E4}	2.5×10^{-5}	μmol/mg dry mass
α_{E10}	2.5×10^{-5}	μmol/mg dry mass
α_{E12}	2.5×10^{-5}	μmol/mg dry mass
Forcing functions		
$V_i = \alpha_V \cdot X$		
$V_o = V_t - \alpha_V \cdot X$		
$E_1 = \alpha_{E1} \cdot X$		
$E_2 = \alpha_{E2} \cdot X$		
$E_3 = \alpha_{E3} \cdot X$		
$E_4 = \alpha_{E4} \cdot X$		
$E_{10} = \alpha_{E10} \cdot X$		
$E_{12} = \alpha_{E12} \cdot X$		

2.3 Rate characteristic of modelling results

The perturbations to the energy *supply* were mimicked by varying the dilution rate in the model (similar to the chemostat experiments which will be discussed in Chapter 4), while the energy demand was modelled by simulating an ATP leak (varying the non-growth consumption of ATP, $[k_{cat10}]$, mimicking the addition of benzoate as uncoupler). (The reasons for the choices of perturbations are explained in greater detail in Chapter 3 on pages 30 and 32). The results obtained were plotted as rate characteristics of ATP supply and demand in double-logarithmic space. Referring to Figure 2.3, the intersection is the reference steady state point where the supply and the demand rates are equal. The elasticities of the supply and the demand with respect to [ATP]/[ADP] can be determined from the slopes to the tangents at the intersection point.

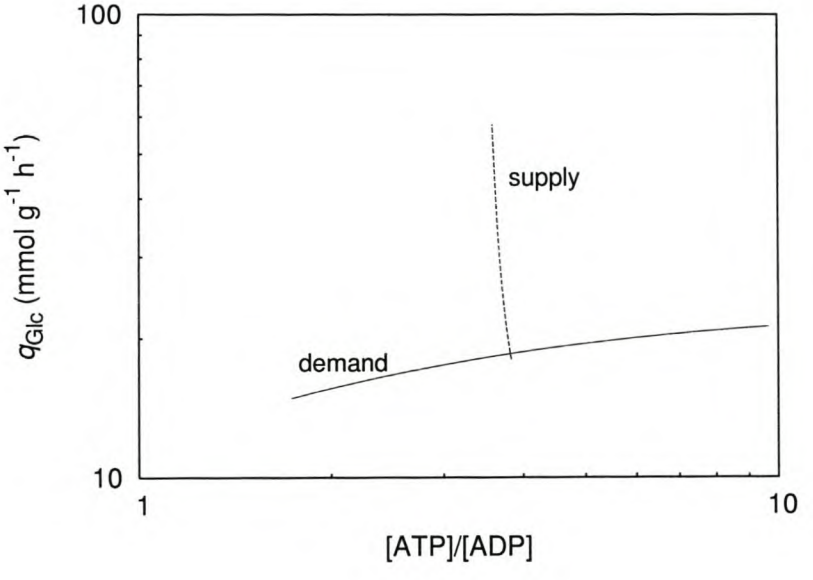

Fig. 2.3 Rate characteristics of ATP supply and demand in the structured kinetic model of yeast growing in an anaerobic chemostat.

The elasticities of the supply $\left(\varepsilon^{\text{supply}}_{atp/adp}\right)$ and demand $\left(\varepsilon^{\text{demand}}_{atp/adp}\right)$ were -8.7 and 0.21 respectively. From these values we could calculate the flux control and con-

centration control coefficients (presented in Table 2.3) using equations 1.11–1.14.

Table 2.3 Flux and concentration control coefficients of the structured kinetic model of anaerobic yeast energy metabolism

C^J_{supply}	C^J_{demand}	$C^{\text{atp/adp}}_{\text{supply}}$	$C^{\text{atp/adp}}_{\text{demand}}$
0.02	0.98	0.11	−0.11

The control pattern observed with the rich media model was similar to the one obtained by Rohwer *et al.* [72] who reported flux control coefficients of the supply and demand as 0.07 and 0.93 respectively.

We continued our investigation by translating the general ideas of the modelling exploration into an experimental setup as set out in Chapter 3.

3 Experimental design

Where possible, the validity of every model should be verified experimentally so we chose *Saccharomyces cerevisiae* as our model organism and supply-demand analysis as our theoretical tool for reasons mentioned previously.

Our aim was to study the control and regulation of anaerobic yeast free-energy metabolism; this chapter describes the translation of our model into an experimental system (independent perturbations of ATP supply and demand reactions and the measurement of the resulting glycolytic fluxes).

3.1 Chemostat cultivation

For our experimental setup the choice fell on anaerobic glucose limited continuous cultures. Chemostats are particularly well suited for the investigation of well defined steady states [85]. The constant growth conditions result in homogeneous yeast morphology and metabolism [5, 86] and the absence of metabolic shifts [7, 86] (e.g. diauxic shifts and respirofermentative growth). We also took advantage of certain chemostat characteristics (e.g. dilution rate) to aid in experimental perturbations as described below.

The yeast was cultivated anaerobically in a chemostat under glucose limitation. When yeast (in this case a *prototrophic* laboratory strain of *S. cerevisiae* to minimize effects of selection pressure [87] and possible physiological complications [6, 9,

88]) is cultivated anaerobically, the fermentation reaction that converts glucose to ethanol and CO_2, is the sole source of ATP. The net reaction can be summarised as follows:

$$\text{glucose} + 2\ \text{ADP} + 2\ P_i \longrightarrow 2\ \text{ethanol} + 2\ CO_2 + 2\ \text{ATP} \tag{3.1}$$

Therefore, in our experimental setup, we considered glucose fermentation as the *supply* of energy, and all growth and maintenance reactions as the *demand*. We used the ratio of the ATP and ADP concentrations ([ATP]/[ADP]) as an indication of the free-energy state of the cell. The use of this ratio is quite permissible as the two concentrations form part of a moiety conserved cycle and only one independent variable exists [55, 89]. Below is a scheme of what we just described in words:

$$\longrightarrow \boxed{\text{Supply}} \longrightarrow \frac{[\text{ATP}]}{[\text{ADP}]} \longrightarrow \boxed{\text{Demand}} \longrightarrow \tag{3.2}$$

3.2 Perturbations

Supply-demand analysis can be applied to scheme 3.2 using the double modulation method described in Chapter 1 on page 11. Practically, this means that perturbations on, e.g., the supply side will cause changes in the [ATP]/[ADP]. These changes in [ATP]/[ADP] are independent relative to the demand side and will be propagated through the rest of the system until a new steady state is reached. Likewise, perturbations on the demand side will cause changes on the supply side flux communicated only through the independent variation in [ATP]/[ADP].

3.2.1 Perturbations on the supply side

Perturbations on the supply side were made by varying the dilution rate D. To understand this concept we have to digress somewhat to remind ourselves of pertinent chemostat theory, referring to Figure 3.1.

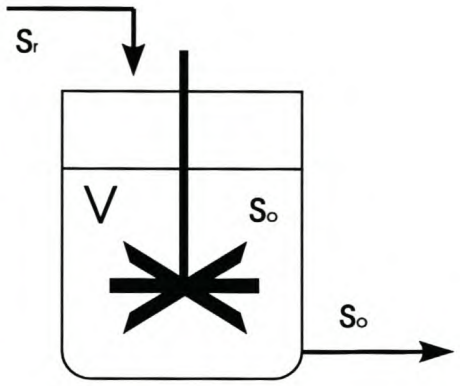

Fig. 3.1 Schematic representation of a chemostat

The dilution rate of a chemostat is the volumetric flow rate F of the medium feed divided by the working volume V with units of h^{-1}.

$$D = \frac{F}{V} \tag{3.3}$$

A mass balance of the growth limiting substrate s around the chemostat looks as follows [90]:

$$\frac{ds}{dt} = D(s_r - s_o) - \frac{\mu x}{Y} \tag{3.4}$$

where s_r and s_o are the molar growth limiting substrate concentration in the medium feed (reservoir) and inside the chemostat respectively. μ is the specific growth rate with units h^{-1}, x is the dry mass concentration of the biomass in g/l and Y is the growth yield (gram biomass/mol substrate). In the steady state $ds/dt = 0$ and $D = \mu$ and equation (3.4) can be rearranged to:

$$x = Y(s_r - s_o) \tag{3.5}$$

From equation (3.5) it is clear that the biomass is directly proportional to $(s_r - s_o)$ assuming constant growth yield. Experimentally we see that the biomass drops slightly with increasing dilution rate. This is due to a slight increase in the growth limiting substrate (glucose) concentration inside the chemostat. An increase in the dilution rate will thus result in a higher glycolytic flux because of the higher

extracellular glucose concentration that the yeast cells are exposed to. Perturbing the dilution rate will therefore result in changes on the supply side.

It is significant that s (glucose) is a *growth limiting* substrate as the validity of equations (3.4) and (3.5) depends on it. For microbial metabolism the free-energy change of catabolic reactions is usually tightly coupled to anabolic steps for growth conditions where the energy source is limiting [91]. Under conditions of energy excess, *S. cerevisiae* also displays uncoupling of catabolic energy production and anabolic energy demands in aerobic and anaerobic continuous cultures [48, 92, 93]. Changes in dilution rate will therefore not alter the catabolic energy supply under conditions of glucose excess.

3.2.2 Perturbations on the demand side

Changes in the demand side are accomplished by titrating with varying concentrations of benzoic acid. The proposed mechanism by which this increased demand for ATP is accomplished was discussed in Chapter 1 on page 5.

At this stage, because S_o is the growth limiting substrate, we assume that its concentration will remain low and rather constant and unaffected with benzoate addition. The validity of this assumption will be addressed in Chapter 5 on page 46.

4 Experimental supply-demand analysis

In this chapter we present results from the data sets of two separate experimental runs. For our first experimental run, we obtained all our data (fluxes and concentrations) from only one sample at each steady state point due to time constraints.

We repeated the experiment in a second run, taking three independent samples at each steady state. Unfortunately unexpected problems were encountered with the ATP and ADP measurements (probably due to different quenching conditions during sampling—refer to page 55). In the latter study it was impossible to draw rate characteristics without knowing the concentrations of ATP and ADP and therefore no further conclusions could be made regarding regulation and control of glycolysis for the second experimental run. However, we do present the primary data obtained from the second experimental run in section 4.3.

4.1 Preparatory experimental controls

4.1.1 Glucose limitation

The importance of glucose limited growth for the perturbations was explained in Chapter 3 on page 32. Taking the pertinent assumptions into account, equation 3.5 shows that the biomass should be proportional to the growth limiting substrate (in

this case glucose). This requirement can easily be verified experimentally by altering only the glucose concentration in the medium feed and determining whether the biomass varies proportionally.

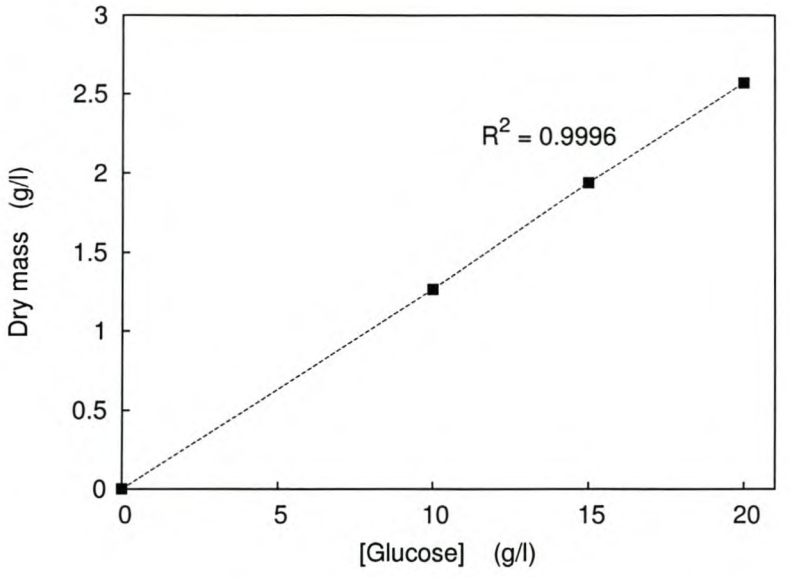

Fig. 4.1 Proportional increase of biomass upon growth limiting substrate (glucose) increase verifies glucose limitation

The results in Figure 4.1 show that we have worked well within the range of glucose limitation for the strain and conditions (10 g/l glucose in feed) used.

4.1.2 Carbon balance and Y_{ATP}

We used a carbon balance to verify whether glucose served solely as the free-energy source and not as a source of carbon intermediates to be incorporated into biomass (in Chapter 2 on page 19, we explained the necessity of this requirement to separate the supply and the demand blocks successfully). To this end, we verified if all the glucose in the medium feed could be accounted for as the products of the energy yielding process of fermentation (ethanol and CO_2). The specific carbon flow rate ($mmol.g^{-1}.h^{-1}$) of the glucose entering the fermentor was compared to the carbon

Table 4.1 Carbon fluxes, q (mmol C.g^{-1}.h^{-1}), from glucose and its recovery as fermentation products (CO_2 and ethanol) at different steady states from the first experimental run.

Steady state	Dry mass	q_{Glc}	q_{CO_2}	C in CO_2	q_{EtOH}	C in EtOH	C recovery
	g/l			%		%	%
D = 0.10 h^{-1}	1.53	22	9	40	12	57	96
D = 0.15 h^{-1}	1.40	36	14	38	22	61	99
D = 0.20 h^{-1}	1.32	51	21	42	31	62	104
D = 0.25 h^{-1}	1.19	70	26	37	45	64	100
D = 0.30 h^{-1}	1.01	101	34	34	59	59	93
[benz] = 1 mM*	0.96	70	24	35	47	67	102
[benz] = 2 mM*	0.71	94	31	34	56	59	93
[benz] = 4 mM*	0.58	116	43	38	78	67	105

*D = 0.2 h^{-1} for the experiments where benzoate was added.

efflux emanating from ethanol and CO_2 (the method of determining CO_2 evolution is described on page 56).

In Table 4.1 the carbon balance is summarised for the different steady states measured (we used HPLC analysis to measure succinate, acetate and glycerol, but the levels were below the limit of detection). The undetectable levels of glycerol probably show that no redox imbalance exist in yeast anaerobic continuous cultures grown on rich media.

Schulze [4], in his studies on anaerobic yeast physiology, found that the molar yield of CO_2 (mole CO_2/mole glucose) is about 9 % higher than the molar yield of ethanol (mole ethanol/mole glucose). He attributed this to the additional formation of CO_2 by processes other than ethanol formation via glycolysis. Albers *et al.* [94] confirmed the results of Schulze (yield of CO_2 about 7 % higher than the ethanol yield on a per mole glucose basis) when they studied the effect of anaerobic yeast in a minimal medium supplemented with a mixture of amino acids. The values of

the CO_2 flux in Table 4.1 are therefore most probably a slight overestimation of purely glycolytic flux, while the ethanol flux will be slightly underestimated due to evaporation. The balance closes within experimental error and thus meets our aim that communication between the supply and demand block should occur only via the linking metabolite.

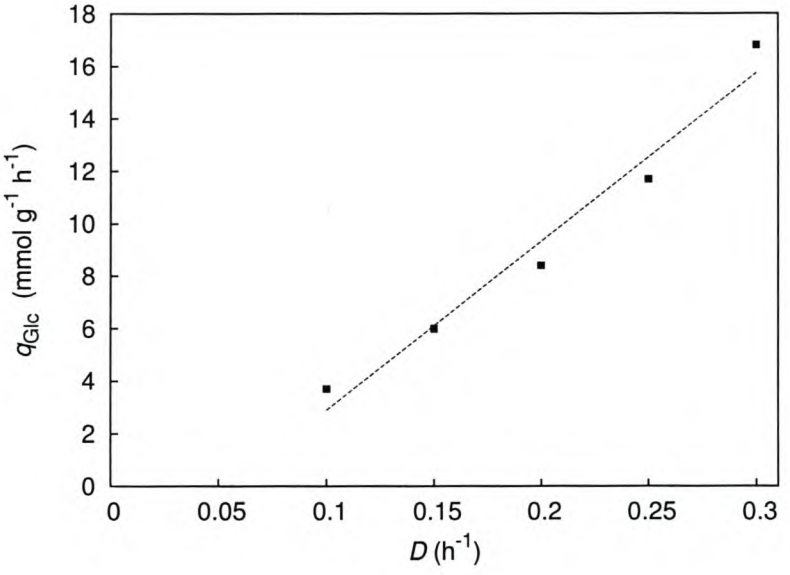

Fig. 4.2 Variation of specific glucose consumption with the dilution rate. (The linear regression line produces a negative intercept on the y-axis and shows that the trend does not hold for low dilution rates. The linearity of the regression line is based on the assumption that the maintenance energy remains constant at the various dilution rates according to Pirt [90]; this is clearly not the case.)

The ATP yield (Y_{ATP}), expressed as gram dry mass formed per mole of ATP produced, can be determined from the slope of in Figure 4.2 [90]. The Y_{ATP} for the first run is 7.8 gram dry mass per mole of ATP based on q_{Glc}. The low value for Y_{ATP} is probably because only one data point was taken at each dilution rate change (e.g. if the data point at $D = 0.3$ is omitted the value of Y_{ATP} becomes 9.4 gram dry mass per mole of ATP which more closely resembles the values reported in literature for anaerobic glucose-limited chemostat cultures [17]).

4.1.3 Antifoam

Most studies on chemostat cultivation reported in the literature were done in defined media, and even with the addition of foam inducers like Tween 80, about 50–75 μl antifoam per liter of medium was sufficient for foam suppression [95, 96] (even at very high stirring speeds (1 000 rpm)). Du Preez *et al.* [97] added yeast extract to their growth medium at a concentration of 3 g/l and used 750 μl antifoam per liter of medium to suppress foam formation in aerated chemostats (i.e. no need for addition of Tween 80).

We found that 250 μl antifoam per liter of rich medium (defined media of Verduyn *et al.* [18] plus 3g/l yeast extract) was sufficient for foam suppression at all the dilution rates investigated at a stirring speed of 400 rpm.

4.2 First experimental run

The results presented in this section have been published as reference [98].

We used ethanol production as an indication of the glycolytic flux. Carbon balances verified that this approach was valid, in that, within experimental error, virtually all the glucose was converted to ethanol and carbon dioxide (see Table 4.1).

Both the change in the dilution rate and titration with benzoic acid had an effect on the glycolytic flux and on the [ATP]/[ADP] ratio. Figure 4.3 shows how glycolytic supply and ATP demand varied with the [ATP]/[ADP] ratio. As a first approximation, we estimated the elasticities by performing a linear regression on the supply and demand data points, yielding values of -0.84 (supply) and 7.2 (demand). From these values the flux- and concentration control coefficients were calculated (see equations 6.4–6.7 for the relationships between elasticity and control coefficients).

In reality, AMP forms part of the adenylate moiety-conserved cycle. We did not measure AMP directly but calculated it from the ATP and ADP concentrations and the adenylate kinase equilibrium constant. Performing the analysis in terms of the charged/uncharged ratio c/u [89], gave very similar values for the elasticities

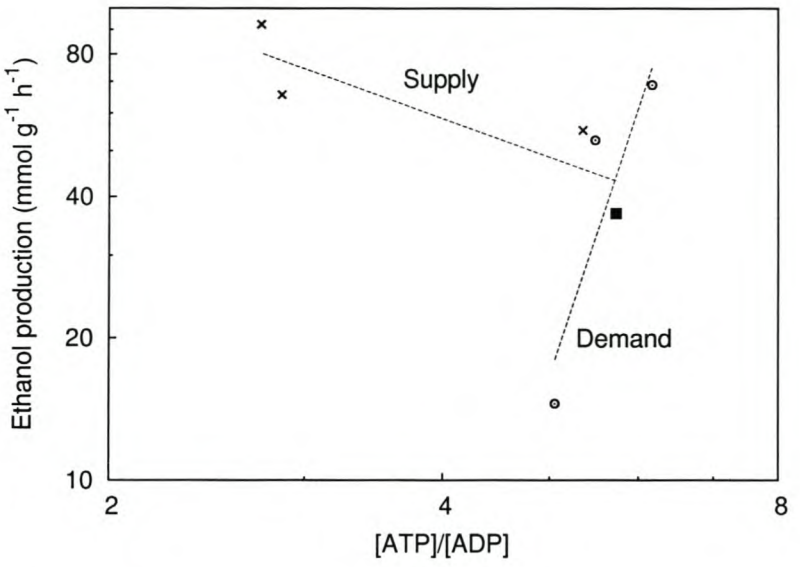

Fig. 4.3 The variation of glycolytic supply and ATP consuming demand in *S. cerevisiae* with the [ATP]/[ADP] ratio. (×) shows the rate characteristic when the ATP demand is modulated (titrating with benzoic acid). (⊙) shows the rate characteristic with perturbations in the supply (changes in dilution rate). (■) is the data point for $D = 0.2\ h^{-1}$ with no benzoic acid added, and is used as the reference point. The dotted lines show the slopes of the rate characteristics, and were calculated by linear regression of the data points.

(−0.78 for the supply and 6.8 for the demand) and control coefficients (Table 4.2).

4.3 Primary data of second experimental run

In this section we present the primary data of the second experimental run. In Figure 4.4 and Figure 4.5, the glycolytic flux is shown to increase linearly with increasing dilution rate and benzoate concentration respectively in agreement with Schulze [4]. It is therefore unfortunate that problems encountered with the ATP and ADP determinations prevented us from constructing the rate characteristics and derive the control structures of the glycolytic flux. The Y_{ATP} for the second run

was 11.0 or 11.4 gram dry mass per mole of ATP based on q_{Glc} or q_{CO_2} respectively, which is higher than for the first run and closer to the literature value of 16 gram dry mass per mole of ATP formed [17].

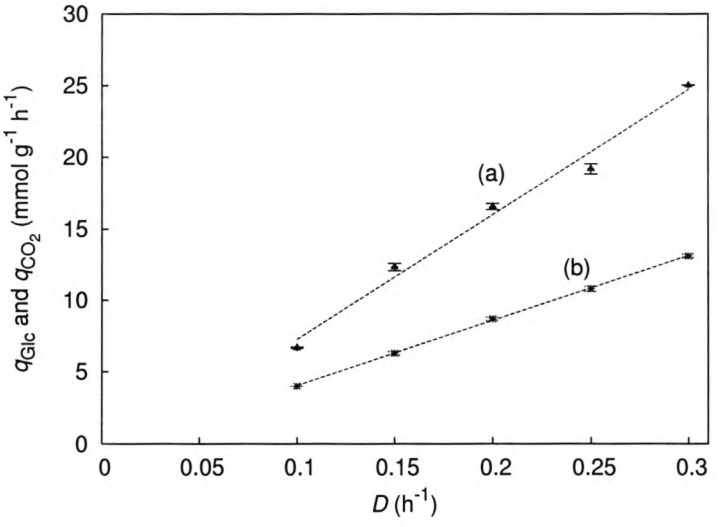

Fig. 4.4 (a) Primary data of specific CO_2 evolution and (b) specific glucose consumption varying with the dilution rate, D for the second run. For each data point three independent steady states were used and error bars reflect the standard error of the mean. (The linear regression line produces a negative intercept on the y-axis and shows that the trend does not hold for low dilution rates.)

Table 4.2 Flux and concentration control coefficients in anaerobic yeast energy metabolism

Linking variable	C^J_{supply}	C^J_{demand}	$C^{\text{link.var.}}_{\text{supply}}$	$C^{\text{link.var.}}_{\text{demand}}$
[ATP]/[ADP]	0.90	0.10	0.12	−0.12
c/u	0.90	0.10	0.13	−0.13

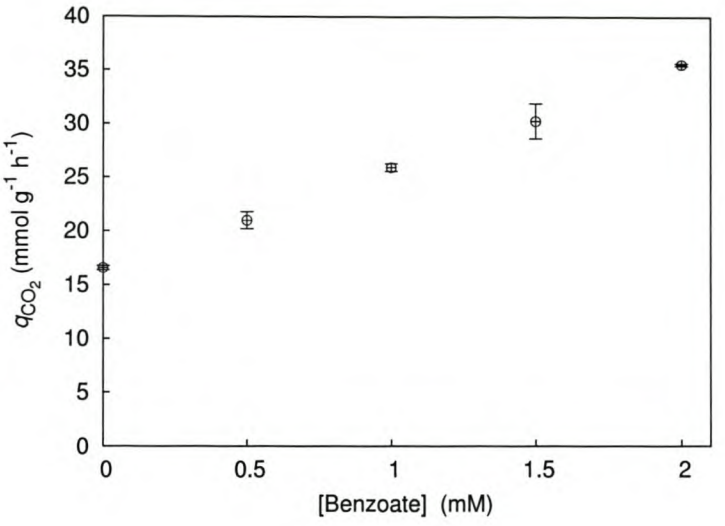

Fig. 4.5 Primary data of CO_2 evolution varying with the benzoate concentration for the second run. For each data point three independent steady states were used and error bars reflect the standard error of the mean

4.4 Discussion

The results presented in section 4.2 are a direct experimental application of the approach to supply-demand analysis advocated by Hofmeyr and Cornish-Bowden [2]. Our results indicate that, under energy-limited low-glucose conditions, the majority of flux control was in the supply. Further, the [ATP]/[ADP] ratio is under strong homeostatic control, as evidenced by the low concentration control coefficients. It is important in this regard to note that our results support the observations of Larsson *et al.* [48, 49], who found a negative correlation of yeast glycolytic flux with ATP concentrations. In our analysis, the "supply" data points (benzoate titration) refer to the properties of glycolysis as a function of [ATP]/[ADP], and here the ethanol production increases with decreasing [ATP]/[ADP]. The "demand" data points refer to the properties of ATP consuming processes, since the perturbation was in the supply block. Hence, the increase in ethanol production with [ATP]/[ADP] upon changing the dilution rate *cannot* be construed as a correlation of *glycolysis* with [ATP]/[ADP].

It could be argued that, since the [NAD^+]/[NADH] ratio also links the supply and demand blocks, this violates the condition that the two blocks should communicate only via a single intermediate. However, we do not expect large changes in the redox ratio for the following two reasons: (i) under all conditions tested, virtually 100 % of the glucose was converted to ethanol, and this is a redox-neutral process; and (ii) this study addresses the supply and demand of ATP (free-energy metabolism), and not of NADH (redox metabolism). Ultimately, we plan to measure NAD^+ and NADH as well, but currently, these data are unavailable. A further criticism might be that uncoupling could affect the transport of building blocks into the cell (and by implication, also perturb the supply). To ensure that this does not affect our analysis, we verified that our culture is glucose (i.e. energy) limited, and not building-block (i.e. carbon) limited, under all experimental conditions tested.

Flux control by the supply contrasts strongly with the results of Schaaff *et al.* [43], who overexpressed a whole series of glycolytic enzymes in yeast (both singly and in combination), only to find absolutely no effect on the glycolytic flux. However, it should be noted that the glucose transport was not included in these studies (see also below). Hofmeyr and Cornish-Bowden [2] took this to suggest that glycolytic flux control lies in the demand for ATP. A possible reason for the discrepancy between their results and ours may be that our experiments were performed under glucose limitation, whereas theirs were in batch culture (i.e., glucose excess). A low glucose concentration would lower the activity of the glucose transporter and confer flux control to it (and consequently to the supply). Indeed, Reijenga *et al.* [47] found experimentally that glucose transport exerts significant control over the average glycolytic flux in glycolytically oscillating yeast incubations, while a detailed kinetic model of yeast glycolysis by Teusink [79] predicts high flux control by the glucose transport step (unpublished results).

In the *Mol. Biol. Rep.* paper [98], we used ethanol production as an indication of the glycolytic flux. Some authors have criticised the use of ethanol to calculate elemental recoveries, because the fraction of ethanol that is stripped depends mainly

on the ratio of the liquid to gaseous flow rates and not so much on low condenser temperature [99]. The evolution of CO_2, however, is an equally suitable way to measure the glycolytic flux. In Figure 4.6 we show that a different (and independently determined) variable (CO_2) used to obtain the rate characteristics, still yield the same control distribution. We used the data set from the same experiments as those published in [98].

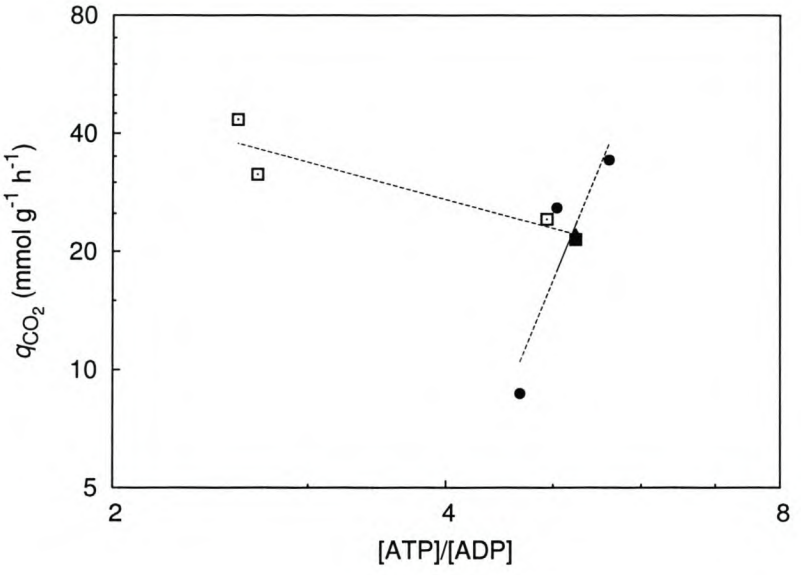

Fig. 4.6 The variation of glycolytic supply and ATP consuming demand in *S. cerevisiae* with the [ATP]/[ADP] ratio, as determined from CO_2 production rates. (⊡) shows the *supply* rate characteristic (titrating with benzoic acid). (•) shows the *demand* rate characteristic (changes in dilution rate). (■) is the data point for $D = 0.2\ h^{-1}$ with no benzoic acid added, and is used as the reference point. The dotted lines show the slopes of the rate characteristics, and were calculated by linear regression of the data points.

A similar graph to Figure 4.6 using ATP concentration rather than [ATP]/[ADP] is represented in Figure 4.7.

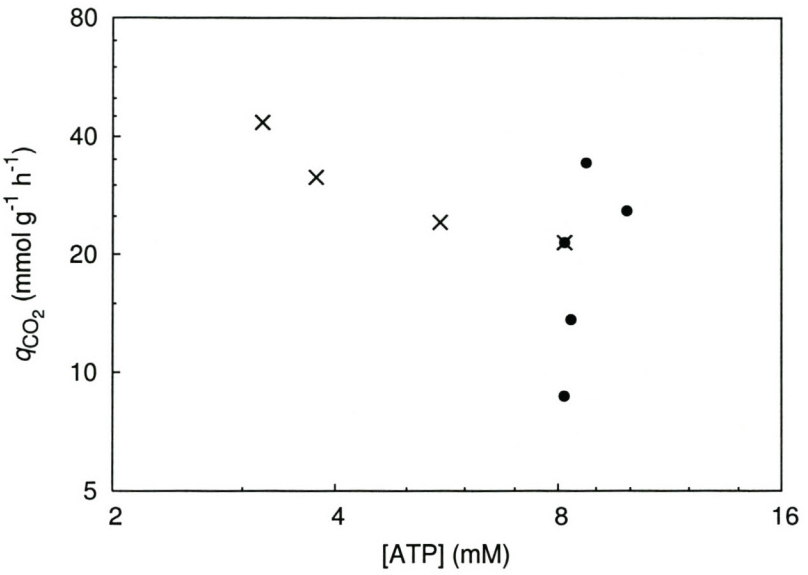

Fig. 4.7 CO_2 evolution varying with the ATP concentration during the first run. (×) shows the *supply* rate characteristic (titrating with benzoic acid). (•) shows the *demand* rate characteristic (changes in dilution rate).

5 General Discussion and Future Perspectives

5.1 Our experimental data in context

The control and regulation of microbial energy metabolism has so many contributing factors that not even extensive review articles manage to address it in its entirety (e.g. [3, 12, 15, 91]). Chapters in books fare slightly better but what they gain in broadness of topic coverage, they loose in depth of content [7].

Instead of trying to answer too many questions at once, we focused our attention on a specific part of energy regulation, i.e. the supply-demand analysis of anaerobic yeast energy metabolism. We combined the approaches of experiments, theoretical frameworks and computer simulations in gaining a clearer understanding of the underlying mechanisms and their interactions.

Some authors have lamented the difficulty of experimental applications to MCA theory [58, 61, 63]. In our case, many precautions were needed like the requirements of steady-state, independent perturbations, no cross talk between the blocks, glucose limitation and closing carbon balances. We agree that our experimental design was a challenge and will benefit from some improvements (see discussion on benzoate below).

Our aim was to determine the control and regulation of anaerobic yeast energy

metabolism applying the tenets of supply-demand analysis. In their theoretical treatment of supply-demand analysis, Hofmeyr and Cornish-Bowden [2] predicted that flux control in the demand (while the supply block determines to which degree the concentration of the linking metabolite, [ATP]/[ADP], is homeostatically maintained) is a solution that might have been taken by many living cells to satisfy the varying demand for a product while maintaining the concentration of these products in a narrow range far from equilibrium. Our results show, however, that flux control resided mainly in the supply for the experimental setup we used, i.e., a glucose-limited anaerobic continuous culture of *S. cerevisiae*. Residual glucose concentrations in glucose limited chemostats are very low [4]. The control of flux in the supply is therefore partly a result of constraints introduced by the system. Koebmann *et al.* [100] also used supply-demand analysis to determine control and regulation of energy metabolism of *Lactococcus lactis* and *Escherichia coli*. They perturbed the linking metabolite, ATP, by introducing uncoupled ATPase activity using molecular genetics. They found in the case of *E. coli*, that ATP demand had almost full control of the flux in contrast with *L. lactis*, where the control of the demand was close to zero. Their results further showed that in non-growing cells of *L. lactis* (which have a low glycolytic flux), the ATP demand *did* have a high flux control. They concluded that the extent to which ATP demand controls glycolytic flux depends on the excess capacity of glycolysis in the cell, as well as the organism and conditions of growth.

One limitation in the current experimental setup is the absence of measurements of residual glucose in the culture vessel. Snoep *et al.* [85] extended classical metabolic control analysis to describe how to determine the control of growth rate in a chemostat. Their analysis shows that it is very important to measure the residual concentration of the growth limiting substrate because of the partial control that it exerts over the growth rate. In the papers by Koebmann *et al.* [100, 101], they refer to studies done in batch cultures (glucose probably present in saturating quantities) and therefore we could not use these data to speculate on a possible

correlation of residual glucose concentration and control of glycolytic flux.

Benzoate as uncoupler may have the added effect of increasing the residual glucose concentration. This would mean that benzoate addition would affect not only the demand side, but also the supply side and violate our double modulation premise that perturbations should communicate only via the linking metabolite. This, however, does not detract from the validity of our results. An increase in flux on the demand side as well as the supply side would result in the data point values of the measured *supply* rate characteristic to be higher than if it were due only to an increase in the demand. The true lower values and resulting lower slope at the intersection point would yield an even higher flux control than reported in Chapter 4 on page 39. In symbols this can be represented as follows: because $\left|\varepsilon_X^{\text{supply (true)}}\right| < \left|\varepsilon_X^{\text{supply (measured)}}\right|$, $C^J_{\text{supply (true)}} > C^J_{\text{supply (measured)}}$ according to equation 1.11.

The choice of [ATP]/[ADP] as linking metabolite deserves further comment adding to the discussion in Chapter 4 (page 40). Earlier work by Larsson *et al.* [48] showed that an increase in glycolytic flux was induced, at a constant growth rate, by changing the conditions from glucose or energy limitation to nitrogen limitation and energy excess. These experiments are similar to perturbations in glycolytic supply and indeed, our results agree with their findings that glycolytic flux decreases with increasing ATP concentration (see Figure 4.7 where the supply is independently perturbed by benzoate additions). Larsson *et al.* [49] report that [ATP]/[ADP] does not influence the glycolytic flux significantly as compared to the inhibitory effect of increasing ATP concentration. In these experiments, ATP and ADP were added to permeabilised cells to study its effect on glycolytic flux *in vivo*. It is, however, difficult to compare these results in a supply-demand context as their addition of external ATP or ADP does not amount to independent perturbations of a linking metabolite, but rather affects the concentration of the total adenine nucleotide pool as well as the [ATP]/[ADP] moiety ratio controlled by adenylate kinase.

5.2 Discussion of model and further modelling results

In addition to a sound theoretical framework and quantitative experimentation, a third leg of our approach was to do computer simulations on a core model of the system we used. Computer simulations are often very helpful in investigations that do not lend themselves to direct experimentation or even in drawing attention to unexpected system behaviour [73]. Rohwer *et al.* [72] found the latter statement to be true in their modelling exploration of the control of free-energy metabolism in yeast. Their model showed that using glucose as the sole carbon and energy source will not allow the application of supply-demand analysis to the system. They therefore suggested the addition of carbon intermediates in the medium feed (for incorporation into biomass) so that all glucose might be used solely as energy source.

The kinetic model described in Chapter 2, however, reveals a different control structure than the experimental results and seems to agree with the postulations of Hofmeyr and Cornish-Bowden [2] that flux control resides in the demand. Under such circumstances it is tempting to agree with Massoud *et al.* [73] when they conclude that:

> ... models satisfy logic when they fail ("but satisfy the lust of the modeller when they succeed !")

However, the value of the scientific exercise would be lost (and would not satisfy logic) if the "failure" of the model to predict the real world system is not at least pondered and discussed.

We therefore started with the same structured kinetic model as before and extended our previous modelling efforts by changing various strategic parameters (e.g. glucose transport into the cell, influence of product inhibition and binding of substrate during transport into the cell) so that the model output better reflected our experimental results. In Table 5.1 we summarise the only differences between

Table 5.1 Comparison of the original and revised kinetic parameters of the enzyme catalysed reactions (All k_{cat} values are in h^{-1} and K_m values in mM). Other parameters as in Table 2.1

Parameter	Original Value	Revised value
Reaction 1: Glucose uptake (facilitated diffusion)		
k_{cat1}	4.0 x 10^6	4.0 x 10^5
$K_{m1(S_o)}$	1	0.1
$K_{m1(S_i)}$	1	0.1
Reaction 2: Glucose converted to product P with ATP production		
k_{cat2}	2.0 x 10^6	7.0 x 10^5
$K_{m2(P_i)}$	1	100
Reaction 3: ATP and yeast extract used in biomass formation		
$K_{m3(\text{ATP})}$	0.1	0.5
$K_{m3(\text{ADP})}$	0.1	0.5

the original and revised model. The supply and demand rate characteristics of the revised model are presented in Figure 5.1.

The elasticities of the supply $\left(\varepsilon_{atp/adp}^{\text{supply}}\right)$ and demand $\left(\varepsilon_{atp/adp}^{\text{demand}}\right)$ at Point B in Fig. 5.1 were -2.0 and 0.17 respectively. From these values we could calculate the flux control and concentration control coefficients (presented in Table 5.2) using equations 1.11–1.14 with X equaling [ATP]/[ADP]. In Table 5.2 we also present the results of the flux and concentration control coefficients if we used $\varepsilon_{atp/adp}^{\text{supply}}$ at Point A (Fig. 5.1) and $\varepsilon_{atp/adp}^{\text{demand}}$ at Point B (Fig. 5.1) to calculate them. We see quite a different control profile with much less control in the demand.

Let us start our discussion with the slope of the demand rate characteristic. In the kinetic model, the slope of this curve was rather insensitive to perturbations of any kind. The form of the supply rate characteristic however, was more susceptible to perturbations. The flattening off of the supply curve towards point A in Figure 5.1 (the slope of the tangent to point A is -0.29) was the result of increased

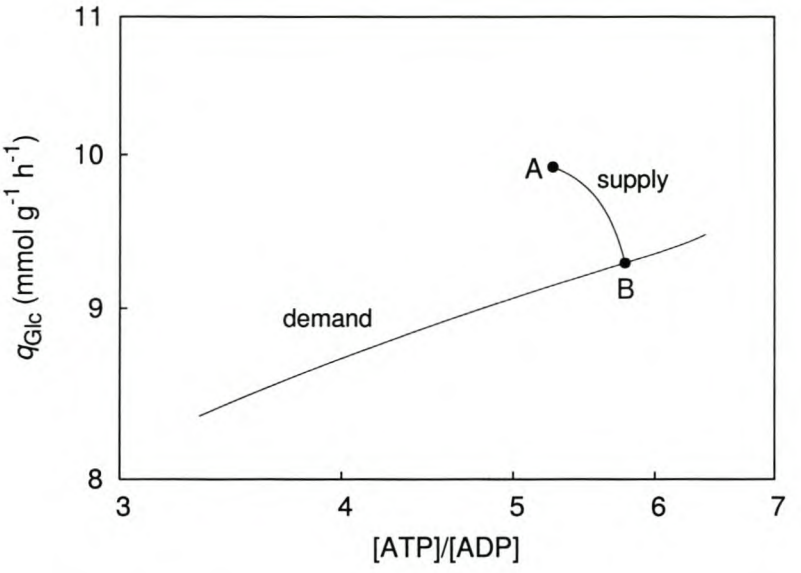

Fig. 5.1 Rate characteristics of ATP supply and demand in the revised structured kinetic model of yeast growing in an anaerobic chemostat. Parameters as in Table 5.1. As for Figure 2.3, the demand curve was generated by varying the parameter D; the supply curve by varying the parameter k_{cat10}. (A and B in the figure merely serve as reference points for discussion to indicate the beginning and end of the supply curve generated by many simulated data points.)

rate limitation of the glucose uptake step—indeed we propose earlier in this chapter that the low glucose concentration in an energy limited chemostat resulted in the experimental control structure we observed.

One could argue that the general form of the supply curve (steep initial slope flattening off as the [ATP]/[ADP] decreases) in the experimental case (Figure 4.3) is the same as the one obtained with modelling (Figure 5.1). The reason for the marked difference in initial values of the slopes of the tangents to the intersection point can be attributed to the difference in the calculation method. In the experimental rate characteristics we calculated the slope with linear regression instead of strictly using the initial slope to the tangent at the intersection point. We used the linear regression as a first approximation because of the lack of sufficient ex-

Table 5.2 Flux and concentration control coefficients of the revised structured kinetic model of anaerobic yeast energy metabolism . Elasticities for the calculation of control coefficients obtained from Figure 5.1

	C^{J}_{supply}	C^{J}_{demand}	$C^{\text{atp/adp}}_{\text{supply}}$	$C^{\text{atp/adp}}_{\text{demand}}$
$\varepsilon^{\text{supply}}_{atp/adp}$ and $\varepsilon^{\text{demand}}_{atp/adp}$ at Point B	0.08	0.92	0.46	−0.46
$\varepsilon^{\text{supply}}_{atp/adp}$ at Point A and $\varepsilon^{\text{demand}}_{atp/adp}$ at Point B	0.36	0.64	2.18	−2.18

perimental data points.

In metabolic control analysis it is permissible to aggregate the elementary fluxes into net fluxes through pools of enzyme catalysed reactions [102] (e.g. glycolysis and growth reaction). De Atauri *et al.* [102] show, however, that flux aggregation can cause the violation of the flux stoichiometry at branch points. This violation of the stoichiometry of fluxes can result in unrealistic steady state concentrations, especially when the control coefficients are assumed to be constant when trying to predict the effect of large changes. In contrast, the perturbations in our model were done in sufficiently small increments to state that *simplistic kinetic rate equations* rather than violation of stoichiometry, had the greatest effect on the calculated control coefficients. Mechanistically the aggregated rate equation (e.g. the reversible two-substrate two-product rate equations with independent binding sites) hardly does justice to the internal regulation hidden in these reactions (glycolysis and growth).

All these findings seem to agree with Palsson and Lee [103], who compared three progressively simpler models of red blood cell metabolism and found no proportionate relationship between the sensitivity coefficients calculated from the three different models (some of the sensitivity coefficients determined by the different models even had opposite signs). They concluded that the model complexity had a significant effect on the values and interpretation of sensitivity coefficients.

Given the simplicity of our structured model, we were able to gain useful insights into the control features of yeast growing in a chemostat. We were able to

verify that the modelled chemostat culture was glucose limited (results not shown) and that the rate limiting nature of the glucose uptake step resulted in the flattening off of the supply rate characteristic. Furthermore, the increasing residual glucose concentration with "benzoate addition" (increasing maintenance component consumption of ATP) was confirmed with the model (results not shown). This phenomenon is anticipated (we have yet to show this experimentally as the residual glucose in the chemostat cultures was not measured) and the consequences are described earlier in this chapter. The variable residual glucose concentration reveals an inability in the current modelling (and experimental) setup to separate the supply and demand blocks cleanly (implications also discussed on page 46). Further refinement of the model may include extending the complexity of the rate equations, (e.g. to incorporate feedback inhibition) and will hopefully result in more mechanistic and dynamic insights in microbial continuous culture growth.

5.3 Future work

Future experiments would include the introduction of rapid sampling methods [104] to measure accurately the residual glucose concentration in the culture vessel in an attempt to quantify the effect it has on the supply block. The glucose consumption rate will also serve as a verification of the glycolytic flux. The question whether excess glucose in the medium feed will in fact result in flux control by demand (as postulated by theoretical studies and predicted by computer simulations) could be verified by perturbing the supply and demand under non-growing conditions. The supply could be perturbed by varying glucose concentrations, which will influence the glycolytic flux without the channelling of excess free energy to biomass formation. In the same way, the demand could be perturbed by benzoate addition. Care should be taken to account for possible glycerol by-product formation.

Another option would be to use different nutrient limitations (e.g. nitrogen)

to obtain a different control distribution between supply and demand (see also [48, 49]). A problem with this approach is that gene expression of the enzymes involved in the free-energy transducing pathways may change as a result of this experimental manipulation, making it hard to separate metabolic and hierarchical control (see below).

It should be emphasised that our results measure the sum of metabolic and hierarchical controls (the control exerted by enzyme synthesis and degradation compared to kinetic and thermodynamic effects of metabolism). Indeed, if the expression levels of one or more of the enzymes involved in yeast energy metabolism change as a result of the perturbations (benzoate addition or dilution rate change), this would affect the control properties of the supply and/or demand blocks and alter the shape of the rate characteristics. This may well be so, in spite of the glycolytic enzymes having no flux control, since their responses to effector molecules may be different. This issue can be addressed by, as a first strategy, determining the total fermentative capacity of the yeast under all our experimental conditions.

In agreement with Koebmann *et al.* [100] we can state in conclusion that the verification of experimental conditions is of utmost importance in any study on control of energy metabolism, whether it is the designing of theoretical frameworks, constructing models or doing experiments. At this stage it seems that there is still no unifying concept to predict the control of energy metabolism for different microorganisms or novel culturing conditions [100]. However, supply-demand metabolic control analysis proved to be a very useful tool to determine experimentally the control structure of energy metabolism for specific organisms and growth conditions.

Finally, this study serves as a paradigm for analysing cellular networks in terms of supply and demand blocks. The analysis can be extended to other pathways.

6 Experimental Procedures

6.1 Yeast culture methods

6.1.1 Yeast strain

All experiments were conducted with the prototrophic CEN.PK113-7D strain of *S. cerevisiae* (obtained from the Free University Amsterdam). Stock cultures were prepared by adding overnight shake-flask cultures to sterile glycerol (final concentration 40 % (V/V)). One milliliter vials of the stock were stored at -80 °C. The shake-flask cultures were grown on YPD medium (OXOID yeast extract, 1 % (m/V); OXOID neutralised bacteriological peptone, 2 % (m/V); D-(+)-glucose (dextrose), 2 % (m/V)) and incubated at 30 °C at 250 rpm.

The strains were maintained [105] on YPD agar plates (OXOID yeast extract, 1 % (m/V); OXOID neutralised bacteriological peptone, 2 % (m/V); dextrose, 2 % (m/V) and Difco agar, 1.5 % (m/V)) at 4 °C for no longer than 6 weeks.

6.1.2 Chemostat cultivation

Anaerobic continuous cultivation was performed at 30 °C in a New Brunswick Bioflo 3000 bioreactor with a working volume of 1.1 litre. The volume of the culture liquid in the chemostat was kept constant with an overflow mechanism that used a peristaltic pump rather than gravity feed. Nitrogen sparging (analytical grade with total

impurities not exceeding 7 ppm) at 0.7 l/min ensured anaerobic conditions and the culture was continuously stirred at 400 rpm with a double Rushton impeller. We used an Inpro 3030 pH electrode from Mettler Toledo and the pH was maintained at 5.0 by automated addition of 2 M KOH. The condensor was kept between 6 and 8 °C with a circulating cooler bath to minimize the loss of ethanol.

6.1.3 Culture media

We used the culture medium described in Verduyn *et al.* [18] with the following modifications: we added ergosterol and Tween 80 dissolved in pure ethanol to final concentrations of 10 mg/l and 420 mg/l respectively to satisfy the anaerobic nutrient requirements of *S. cerevisiae*. Silicon antifoam (Sigma) with a final concentration of 250 μl per litre suppressed foam formation, which became especially problematic at dilution rates above 0.2 h^{-1}. The source of carbon intermediates was yeast extract (OXOID), added to a final concentration of 3 g/l and the energy source was dextrose (Sigma) at 10 g/l. In this medium, the strain exhibited a μ_{max} of 0.42 h^{-1}, growing exponentially in batch culture.

The medium vessels with the buffer salts and mineral supplements and the antifoam were sterilised by autoclaving at 121 °C for one and a half hours. We autoclaved the dextrose and yeast extract separately at 110 °C for half an hour to avoid caramelisation. The filter sterilised vitamin stock solution as well as the ergosterol/Tween 80 were added under sterile conditions.

In the instances of benzoate addition, it was autoclaved with the medium as sodium benzoate at the appropriate final concentrations.

6.2 Sampling, dry mass and metabolite analysis

We defined a steady state when the surveillance variables (dry mass, ethanol concentration and CO_2 evolution) would be constant within 5 % for three samples, each taken at least three residence times apart. For the results of the first run presented

in Chapter 4 on page 38, we assumed a steady state occurred after a period of five or more residence times following a perturbation [4]. At each sampling opportunity the sample was split in three parts. One part of the sample was set aside for dry mass determination. The second part was collected in a pre-cooled vial for HPLC analysis and kept on ice to prevent the loss of ethanol. It was centrifuged in an Eppendorf Centifuge 5804 R at 20800 $\times$ g and 4 °C for five minutes. The third part of the sample was used to determine the intracellular ATP and ADP concentrations. It was withdrawn from the chemostat into a vial with 8 ml chilled 10 % perchloric acid (PCA) in a ratio of one part sample to one part PCA and incubated on ice for 10 minutes. The exact volume of the sample was determined by weighing the vial before and after the addition of the sample. Subsequently we neutralised the quenched sample by slowly adding 4 ml chilled 2 M K_2CO_3 and incubating it on ice for a further 10 minutes. The neutralised sample was clarified in an Eppendorf Centifuge 5804 R at 20800 $\times$ g and 4 °C for five minutes to remove the precipitated salts and proteins. The supernatant of both parts two and three was then stored at −20 °C until the various metabolite concentrations could be determined.

6.2.1 Dry mass determination

We used the method for dry mass determination described by Schulze [4] in duplicate. A cellulose acetate filter (pore size, 0.22 μm; OSMONICS) was dried in a Daewoo KOR-9515 microwave oven at ± 330 W (defrost) for 4 minutes. The filter was cooled in a desiccator and weighed. A known volume of culture liquid (10 ml) was filtered and washed with demineralised water to remove the medium salts. The filter was then dried in the microwave for 8 minutes at the same power setting as before, cooled in a desiccator and weighed.

6.2.2 Ethanol, glycerol, succinate and acetate concentrations determined with HPLC

The concentrations of glucose, ethanol, glycerol, succinate and acetate were measured by means of an HPLC system with pumps, oven and detectors from Knauer. We used an Aminex HPX·87H ion exclusion column from BIO-RAD. The column temperature was kept constant at 55 °C while it was isocratically eluted with 10 mM degassed H_2SO_4 at a flow rate of 0.5 ml/min. The detection unit consisted of a spectrophotometer for UV detection at 210 nm and a refractive index detector.

HPLC sample pre-treatment: The supernatant that was previously prepared was incubated on ice for 10 minutes with PCA added to a final concentration of 2 % (m/m). After the first incubation period we added KOH to a final concentration of 0.333 M and incubated for a further 10 minutes on ice. The solution was then centrifuged at $20800 \times g$ for 5 minutes at 4 °C to remove the precipitated salts and proteins. The supernatant was filtered with 0.22 μm Durapore (Millipore) filters and injected onto the HPLC column.

The HPLC readings were obtained from linear standard curves of glucose, ethanol, glycerol, acetate and succinate that was set up over a range of 5 mM to 100 mM. We used the peak areas as opposed to Schulze [4] who found better linearity and lower relative standard deviation with peak hights.

6.2.3 CO_2 evolution

We measured the CO_2 concentration in the chemostat exhaust gas with a 1313 Fermentation Monitor from INNOVA. It is a combined magnetoacoustic/photoacoustic gas analyser [4] where the measurements are given as a volumetric percentage of the total gas flow referenced to dry gas conditions. These values were converted to molar flow rates assuming ideal gas properties.

The CO_2 leaving the reactor via the condensor can therefore be calculated from

$$F_{CO_2} = \frac{y_{CO_2} \cdot F_{gas}}{V_M} \tag{6.1}$$

where F_{CO_2} is the molar flow rate of CO_2 in the exhaust gas in (mmol/h), y_{CO_2} is the mole fraction of CO_2 in the exhaust gas (measurement of the Fermentation Monitor), F_{gas} is the total flow rate of gas sparged through the reactor (l/h), and V_M is the molar volume (l/mmol) calculated from the ideal gas law at 22 °C and atmospheric pressure.

6.2.4 ATP and ADP concentrations determined with bioluminescence

ATP in the solution was quantitatively measured by an ATP Bioluminescence Assay Kit CLS II from Roche that uses the luciferase enzyme to emit light upon conversion of luciferin to oxyluciferin with the concomitant hydrolysis of ATP to AMP.

The light emission follows a Michaelis-type of equation. At low ATP concentrations ([ATP] $\ll K_m$) the light output becomes directly proportional to the ATP concentration. We used a BioOrbit 1253 luminometer to measure the amount of light emitted.

The amount of ADP present was measured by converting it to ATP with a coupling reaction that uses pyruvate kinase (PK) to convert phoshoenolpyruvate (PEP) to pyruvate.

$$\text{ADP} + \text{PEP} \xrightarrow[(Mg^{2+}, K^{+})]{\text{PK}} \text{ATP} + \text{pyruvate}$$

We used PEP from Sigma as it contains no ADP. If the PEP contained ADP (as is the case with other suppliers), additional controls would be necessary to distinguish the background signal from the ADP in the sample. The pyruvate kinase from Roche was made glycerol free by exchanging the glycerol with the ATP buffer using a mini spin column packed with a Sephadex G-50 slurry.

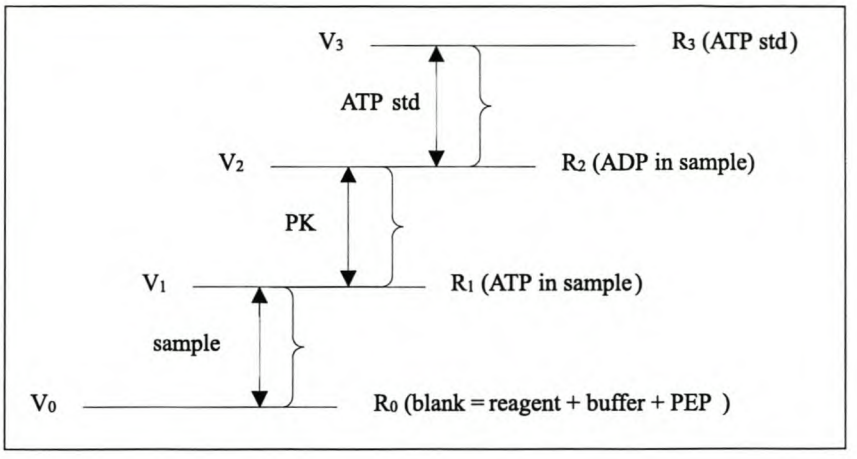

Fig. 6.1 Schematic diagram of the additions and readings of the ATP bioluminescence assay

Additions to luminometer cuvette: To a luminometer cuvette we added 200 μl buffer, 40 μl luciferase reagent and 5 μl PEP (200 mM) and measured the background. The buffer consisted of 100 mM Tris, 10 mM K-acetate, 2 mM EDTA and 10 mM $MgCl_2$ at a pH of 7.75. We added 5 μl sample that we prepared previously and waited until the signal became stable and measured the $(ATP)_{sample}$ signal (R_1). To determine the ADP content in the sample we added 5 μl pyruvate kinase, waited until the signal became stable and measured the $(ATP + ADP)_{sample}$ signal (R_2). An internal ATP standard was added as 5 μl of a 1 μM ATP solution. We waited until the signal became stable and measured the $((ATP + ADP)_{sample} + (ATP)_{standard})$ signal (R_3).

Corrections for dilution effects

The BioOrbit 1253 luminometer uses a side window type photon multiplier tube (PMT) detection unit. It measures *concentrations* of light which means that when buffer is added, a dilution of the ATP will take place, and the measured signal will be lowered. To correct for this dilution one has to add to the signal after addition, the signal before addition multiplied by the fraction of loss due to dilution.

Corrected readings ($R^{'}$) were calculated using V_0 as the reference volume.

$$\begin{aligned} R_1^{'} &= \frac{V_1}{V_0} \cdot R_1 \\ R_2^{'} &= \frac{V_2}{V_0} \cdot R_2 \\ R_3^{'} &= \frac{V_3}{V_0} \cdot R_3 \end{aligned}$$

From figure 6.1 and the description above it is clear that the $(\text{ATP})_{\text{sample}}$ signal is given by $(R_1^{'} - R_0^{'})$. The $(\text{ADP})_{\text{sample}}$ signal is given by $(R_2^{'} - R_1^{'})$ and the signal because of the ATP standard is given by $(R_3^{'} - R_2^{'})$. For our assays $V_1 - V_0 = V_3 - V_2 = 5\ \mu\text{l}$ and therefore both equations 6.2 and 6.3 reduce to their final form.

To calculate the absolute concentration of ATP in the sample, relative to the ATP standard,

$$\begin{aligned} [\text{ATP}]_{\text{sample}} &= \frac{\frac{R_1^{'} - R_0^{'}}{V_1 - V_0}}{\frac{R_3^{'} - R_2^{'}}{V_3 - V_2}} \times [\text{ATP standard } (1\ \mu\text{M})] \\ &= \frac{R_1^{'} - R_0^{'}}{R_3^{'} - R_2^{'}} \times [\text{ATP standard } (1\ \mu\text{M})] \end{aligned} \tag{6.2}$$

To calculate the absolute concentration of ADP in the sample, relative to the ATP standard,

$$\begin{aligned} [\text{ADP}]_{\text{sample}} &= \frac{\frac{R_2^{'} - R_1^{'}}{V_1 - V_0}}{\frac{R_3^{'} - R_2^{'}}{V_3 - V_2}} \times [\text{ATP standard } (1\ \mu\text{M})] \\ &= \frac{R_2^{'} - R_1^{'}}{R_3^{'} - R_2^{'}} \times [\text{ATP standard } (1\ \mu\text{M})] \end{aligned} \tag{6.3}$$

6.2.5 Calculation of control coefficients

From the slopes of the tangents to the double logarithmic rate characteristic at the reference steady state point (see e.g. Figure 4.3), we calculated the elasticities and control coefficients [2] using the following equations:

$$C^{J}_{\text{supply}} = \frac{\varepsilon^{\text{demand}}_{atp/adp}}{\varepsilon^{\text{demand}}_{atp/adp} - \varepsilon^{\text{supply}}_{atp/adp}} \tag{6.4}$$

$$C^{J}_{\text{demand}} = \frac{-\varepsilon^{\text{supply}}_{atp/adp}}{\varepsilon^{\text{demand}}_{atp/adp} - \varepsilon^{\text{supply}}_{atp/adp}} \tag{6.5}$$

$$C^{atp/adp}_{\text{supply}} = \frac{1}{\varepsilon^{\text{demand}}_{atp/adp} - \varepsilon^{\text{supply}}_{atp/adp}} \tag{6.6}$$

$$C^{atp/adp}_{\text{demand}} = \frac{-1}{\varepsilon^{\text{demand}}_{atp/adp} - \varepsilon^{\text{supply}}_{atp/adp}} \tag{6.7}$$

7 Bibliography

[1] Cascante, M. & Martí, E. (1997) Organization and regulation of the metabolic factory, in *New Beer in an Old Bottle: Eduard Buchner and the Growth of Biochemical Knowledge* (Cornish-Bowden, A., ed.), Col.lecció Oberta, pp. 199–214, Universitat de València, Valencia.

[2] Hofmeyr, J.-H. S. & Cornish-Bowden, A. (2000) Regulating the cellular economy of supply and demand, *FEBS Lett. 476*, 47–51.

[3] Flores, C.-L., Rodríguez, C., Petit, T. & Gancedo, C. (2000) Carbohydrate and energy-yielding metabolism in non-conventional yeasts, *FEMS Microbiol. Rev. 24*, 507–529.

[4] Schulze, U. (1995) *Anaerobic physiology of* Saccharomyces cerevisiae, Ph.D. thesis, Technical University of Denmark.

[5] Visser, W., van Spronsen, E. A., Nanninga, N., Pronk, J. T., Kuenen, J. G. & van Dijken, J. P. (1995) Effects of growth conditions on mitochondrial morphology in *Saccharomyces cerevisiae*, *Anton. Leeuw. 67*, 243–253.

[6] Pronk, J. T., Steensma, H. Y. & van Dijken, J. P. (1996) Pyruvate metabolism in *Saccharomyces cerevisiae*, *Yeast. 12*, 1607–1633.

[7] Walker, G. M. (1998) *Yeast physiology and biotechnology*, John Wiley and Sons, New York.

[8] Kurtzman, C. P. & Fell, J. W. (1998) *The yeasts. A taxonomic study*, Elsevier Science, Amsterdam.

[9] van Dijken, J. P., Bauer, J., Brambilla, L., Duboc, P., Francois, J. M., Gancedo, C., Giuseppin, M. L. F., Heijnen, J. J., Hoare, M., Lange, H. C., Madden, E. A., Niederberger, P., Nielsen, J., Parrou, J. L., Petit, T., Porro, D., Reuss, M., van Riel, N., Rizzi, M., Steensma, H. Y., Verrips, C. T., Vindeløv, J. & Pronk, J. T. (2000) An interlaboratory comparison of physiological and genetic properties of four *Saccharomyces cerevisiae* strains, *Enzyme Microb. Technol. 26*, 706–714.

[10] Wheals, A. E., Basso, L. C., Alves, D. M. G. & Amorim, H. V. (1999) Fuel ethanol after 25 years, *TIBTECH 17*, 482–487.

[11] Wang, Z., Zhuge, J., Fang, H. & Prior, B. A. (2001) Glycerol production by microbial fermentation: A review, *Biotechnol. Adv. 19*, 201–223.

[12] Alexander, M. A. & Jeffries, T. W. (1990) Respiratory efficiency and metabolite partitioning as regulatory phenomena in yeasts, *Enzyme Microb. Technol. 12*, 2–19.

[13] Postma, E., Verduyn, C., Scheffers, W. A. & van Dijken, J. P. (1989) Enzymic analysis of the Crabtree effect in glucose-limited chemostat cultures of *Saccharomyces cerevisiae*, *Appl. Environ. Microb. 55*, 468–477.

[14] van Hoek, P., van Dijken, J. P. & Pronk, J. T. (2000) Regulation of fermentative capacity and levels of glycolytic enzymes in chemostat cultures of *Saccharomyces cerevisiae*, *Enzyme Microb. Technol. 26*, 724–736.

[15] Verduyn, C. (1991) Physiology of yeasts in relation to biomass yields, *Anton. Leeuw. 60*, 325–553.

[16] Verduyn, C., Postma, E., Scheffers, W. A. & van Dijken, J. P. (1990) Physiology

of *Saccharomyces cerevisiae* in anaerobic glucose-limited chemostat cultures, *J. Gen. Microbiol. 136*, 395–403.

[17] Verduyn, C., Postma, E., Scheffers, W. A. & van Dijken, J. P. (1990) Energetics of *Saccharomyces cerevisiae* in anaerobic glucose-limited chemostat cultures, *J. Gen. Microbiol. 136*, 405–412.

[18] Verduyn, C., Postma, E., Scheffers, W. A. & van Dijken, J. (1992) Effect of benzoic acid on metabolic fluxes in yeasts: A continuous-culture study on the regulation of respiration and alcoholic fermentation, *Yeast 8*, 501–517.

[19] Visser, W., Scheffers, W. A., Batenburg-Van der Vegte, W. H. & van Dijken, J. P. (1990) Oxygen requirements of yeasts, *Appl. Environ. Microb. 56*, 3785–3792.

[20] Andreasen, A. A. & Stier, T. J. B. (1953) Anaerobic nutrition of *Saccharomyces cerevisiae* I. Ergosterol requirement for growth in a defined medium, *J. Cell. Comp. 41*, 23–26.

[21] Andreasen, A. A. & Stier, T. J. B. (1954) Anaerobic nutrition of *Saccharomyces cerevisiae* II. Unsaturated fatty acid requirement for growth in a defined medium, *J. Cell. Comp. 43*, 271–281.

[22] Parks, L. W. (1995) Physiological implications of sterol biosynthesis in yeast, *Annu. Rev. Microbiol. 49*, 95–116.

[23] Bisson, L. F. (1999) Stuck and sluggish fermentations, *Am. J. Enol. Viticult. 50*, 107–119.

[24] Lubbers, S., Verret, C. & Voilley, A. (2001) The effect of glycerol on the perceived aroma of a model wine and a white wine, *Lebensm.-Wiss. Technol. 34*, 262–265.

[25] Pasteur, L. (1861) Experiments and new views on the nature of fermentations, *Comptes Rendus 52*, 1260.

[26] Jones, R. P. & Greenfield, P. F. (1982) Effect of carbon dioxide on yeast growth and fermentation, *Enzyme Microb. Technol. 4*, 210–223.

[27] de Kock, S. H., du Preez, J. C. & Killian, S. G. (2000) The effect of vitamins and amino acids on glucose uptake in aerobic chemostat cultures of three *Saccharomyces cerevisiae* strains, *System. Appl. Microbiol. 23*, 41–46.

[28] Carlson, M. (1999) Glucose repression in yeast, *Curr. Opin. Microbiol. 2*, 202–207.

[29] Gancedo, J. M. (1998) Yeast carbon catabolite repression, *Microbiol. Mol. Biol. Rev. 62*, 334–361.

[30] Sierkstra, L. N., Verbakel, J. M. A. & Verrips, C. T. (1992) Analysis of transcription and translation of glycolytic enzymes in glucose-limited continuous cultures of *Saccharomyces cerevisiae*, *J. Gen. Microbiol. 138*, 2559–2566.

[31] van Urk, H., Mak, P. R., Scheffers, W. A. & van Dijken, J. P. (1988) Metabolic responses of *Saccharomyces cerevisiae* CBS 8066 and *Candida utilis* CBS 621 upon transition from glucose limitation to glucose excess, *Yeast. 4*, 283–291.

[32] van Hoek, P., Flikweert, M. T., van der Aart, Q. J. M., Steensma, H. Y., van Dijken, J. P. & Pronk, J. T. (1998) Effects of pyruvate decarboxylase overproduction on flux distribution at the pyruvate branch point in *Saccharomyces cerevisiae*, *Appl. Environ. Microb. 64*, 2133–2140.

[33] Flikweert, M. T., Kuyper, M., van Maris, A. J. A., Kötter, P., van Dijken, J. P. & Pronk, J. T. (1999) Steady-state and transient-state analysis of growth and metabolite production in a *Saccharomyces cerevisiae* strain with reduced pyruvate-decarboxylase activity, *Biotechnol. Bioeng. 66*, 42–50.

[34] Aiba, S., Shoda, M. & Nagatani, M. (2000) Kinetics of product inhibition in alcohol fermentation, *Biotechnol. Bioeng. 67*, 671–690.

[35] Björkqvist, S., Ansell, R., Adler, L. & Lidén, G. (1997) Physiological response to anaerobicity of glycerol-3-phosphate dehydrogenase mutants of *Saccharomyces cerevisiae*, *Appl. Environ. Microb. 63*, 128–132.

[36] Påhlman, I.-L., Gustafsson, L., Rigoulet, M. & Larsson, C. (2001) Cytosolic redox metabolism in aerobic chemostat cultures of *Saccharomyces cerevisiae*, *Yeast 18*, 611–620.

[37] Michnick, S., Roustan, J.-L., Remize, F., Barre, P. & Dequin, S. (1997) Modulation of glycerol and ethanol yields during alcoholic fermentation in *Saccharomyces cerevisiae* strains overexpressed or disrupted for *GPD1* encoding glycerol 3-phosphate dehydrogenase, *Yeast 13*, 783–793.

[38] Ansell, R., Granath, K., Hohmann, S., Thevelein, J. M. & Adler, L. (1997) The two isoenzymes for yeast NAD^+-dependent glycerol 3-phosphate dehydrogenase encoded by *GDP1* and *GDP2* have distinct roles in osmoadaptation and redox regulation, *EMBO J. 16*, 2179 - 2187.

[39] Diderich, J. A., Schepper, M., van Hoek, P., Luttik, M. A. H., van Dijken, J. P., Pronk, J. T., Klaassen, P., Boelens, H. F. M., de Mattos, M. J. T., van Dam, K. & Kruckeberg, A. L. (1999) Glucose uptake kinetics and transcription of *HXT* genes in chemostat cultures of *Saccharomyces cerevisiae*, *J. Biol. Chem. 274*, 15350–15359.

[40] Cortassa, S. & Aon, M. A. (1997) Distributed control of the glycolytic flux in wild-type cells and catabolite repression mutants of *Saccharomyces cerevisiae* growing in carbon-limited chemostat cultures, *Enzyme Microb. Technol. 21*, 596–602.

[41] Postma, E., Scheffers, W. A. & van Dijken, J. P. (1989) Kinetics of growth and glucose transport in glucose-limited chemostat cultures of *Saccharomyces cerevisiae* CBS 8066, *Yeast 5*, 159–165.

[42] Müller, S., Zimmermann, F. K. & Boles, E. (1997) Mutant studies of phosphofructo-2-kinases do not reveal an essential role of fructose-2,6- bisphosphate in the regulation of carbon fluxes in yeast cells, *Microbiology 143*, 3055–3061.

[43] Schaaff, I., Heinisch, J. & Zimmermann., F. (1989) Overproduction of glycolytic enzymes in yeast, *Yeast 5*, 285–290.

[44] Kacser, H. & Burns, J. A. (1973) The control of flux, *Symp. Soc. Exp. Biol. 27*, 65–104.

[45] Fell, D. (1997) *Understanding the control of metabolism*, Portland Press, London.

[46] Ye, L., Kruckeberg, A. L., Berden, J. A. & van Dam, K. (1999) Growth and glucose repression are controlled by glucose transport in *Saccharomyces cerevisiae* cells containing only one glucose transporter, *J. Bacteriol. 181*, 4673–4675.

[47] Reijenga, K., Snoep, J., Diderich, J., Verseveld, H. V., Westerhoff, H. & Teusink, B. (2001) Control of glycolytic dynamics by hexose transport in *Saccharomyces cerevisiae*, *Biophys. J. 80*, 626–634.

[48] Larsson, C., Nilsson, A., Blomberg, A. & Gustafsson, L. (1997) Glycolytic flux is conditionally correlated with ATP concentration in *Saccharomyces cerevisiae*: a chemostat study under carbon- or nitrogen-limiting conditions, *J. Bacteriol. 179*, 7243–7250.

[49] Larsson, C., Påhlman, I.-L. & Gustafsson, L. (2000) The importance of ATP as a regulator of glycolytic flux in *Saccharomyces cerevisiae*, *Yeast 16*, 797–809.

[50] Galazzo, J. L. & Bailey, J. E. (1990) Fermentation pathway kinetics and metaboic flux control in suspended and immobilized *Saccharomyces cerevisiae*, *Enzyme Microb. Technol. 12*, 162–172.

[51] Korzeniewski, B. (1999) Theoretical studies on how ATP supply meets ATP demand, *Biochem. Soc. Trans. 27*, 271–276.

[52] Thomas, S. & Fell, D. A. (1998) A control analysis exploration of the role of ATP utilisation in glycolytic-flux control and glycolytic-metabolite-concentration regulation, *Eur. J. Biochem. 258*, 956–967.

[53] Cornish-Bowden, A., Hofmeyr, J.-H. S. & Cárdenas, M. L. (1995) Strategies for manipulating metabolic fluxes in biotechnology, *Bioorg. Chem. 23*, 439–449.

[54] Hofmeyr, J.-H. S. & Cornish-Bowden, A. (1991) Quantitative assessment of regulation in metabolic systems, *Eur. J. Biochem. 200*, 223–236.

[55] Hofmeyr, J.-H. S. (1997) Anaerobic energy metabolism in yeast as a supply-demand system, in *New Beer in an Old Bottle: Eduard Buchner and the Growth of Biochemical Knowledge* (Cornish-Bowden, A., ed.), Col.lecció Oberta, pp. 225–242, Universitat de València, Valencia.

[56] Kacser, H., Burns, J. A. & Fell, D. A. (1995) The control of flux: 21 years on, *Biochem. Soc. Trans. 23*, 341–366.

[57] Heinrich, R. & Rapoport, T. A. (1974) A linear steady-state treatment of enzymatic chains. General properties, control and effector strength, *Eur. J. Biochem. 42*, 89–95.

[58] Fell, D. A. (1992) Metabolic control analysis: a survey of its theoretical and experimental development, *Biochem. J. 286*, 313–330.

[59] Hofmeyr, J.-H. S. & Cornish-Bowden, A. (1996) Co-response analysis: A new experimental strategy for metabolic control analysis, *J. Theor. Biol. 182*, 371–380.

[60] Kacser, H. & Burns, J. A. (1979) Molecular democracy: who shares the controls?, *Biochem. Soc. Trans. 7*, 1149–1160.

[61] Brown, G. C., Hafner, R. P. & Brand, M. D. (1990) A 'top-down' approach to the determination of control coefficients in metabolic control theory, *Eur. J. Biochem. 188*, 321–325.

[62] Brand, M. D. (1996) Top down metabolic control analysis, *J. Theor. Biol. 182*, 351–360.

[63] Quant, P. A. (1993) Experimental application of top-down control analysis to metabolic systems, *Trends Biochem. Sci. 18*, 26–30.

[64] Ainscow, E. K. & Brand, M. D. (1995) Top-down control analysis of systems with more than one common intermediate, *Eur. J. Biochem. 231*, 579–586.

[65] Ainscow, E. K. & Brand, M. D. (1998) Contol analysis of systems with reaction blocks that 'cross-talk', *Biochim. Biophys. Acta 1366*, 284 – 290.

[66] Kahn, D. & Westerhoff, H. V. (1991) Control theory of regulatory cascades, *J. Theor. Biol. 153*, 255–285.

[67] Schuster, S., Kahn, D. & Westerhoff, H. V. (1993) Modular analysis of the control of complex metabolic pathways, *Biophys. Chem. 48*, 1–17.

[68] Westerhoff, H. V. & van Dam, K. (1987) *Thermodynamics and Control of Biological Free-Energy Transduction*, Elsevier, Amsterdam.

[69] Hofmeyr, J. H. S. & Westerhoff, H. V. (2001) Building the cellular puzzle - Control in multi-level reaction networks, *J. Theor. Biol. 208*, 261–285.

[70] Samuelson, P. A. & Nordhaus, W. D. (1992) *Economics*, McGraw-Hil, Singapore, 14th edn.

[71] Hofmeyr, J. H. S. (1995) Metabolic regulation: a control analytic perspective., *J. Bioenerg. Biomembr. 27*, 479–490.

[72] Rohwer, J. M., Hoorneman, M., Hofmeyr, J.-H. S. & Snoep, J. L. (2000) Assessing the control of fermentative free-energy metabolism in yeast: a modelling exploration, in *Animating the Cellular Map: Proceedings of the 9th International Meeting on BioThermoKinetics, Stellenbosch* (Hofmeyr, J.-H., Rohwer, J. M. & Snoep, J. L., eds.) pp. 213–219, Stellenbosch University Press, Stellenbosch.

[73] Massoud, T. F., Hademenos, G. J., Young, W. L., Gao, E. Z., Pile-Spellman, J. & Viñuela, F. (1998) Principles and philosophy of modeling in biomedical research, *Faseb J. 12*, 275–285.

[74] Wiechert, W. (2002) Modeling and simulation: tools for metabolic engineering, *J. Biotechnol. 94*, 37–63.

[75] Duboc, P., von Stockar, U. & Villadsen, J. (1998) Simple generic model for dynamic experiments with *Saccharomyces cerevisiae* in continuous culture: Decoupling between anabolism and catabolism, *Biotechnol. Bioeng. 60*, 180–189.

[76] Lei, F., Rotbøll, M. & Jørgensen, S. B. (2001) A biochemically structured model for *Saccharomyces cerevisiae*, *J. Biotechnol. 88*, 205–221.

[77] Hynne, R., Danø, S. & Sørensen, P. G. (2001) Full-scale model of glycolysis in *Saccharomyces cerevisiae*, *Biophys. Chem. 94*, 121–163.

[78] Rizzi, M., Baltes, M., Theobald, U. & Reuss, M. (1997) In vivo analysis of metabolic dynamics in *Saccharomyces cerevisiae*: II. Mathematical model, *Biotechnol. Bioeng. 55*, 592–608.

[79] Teusink, B., Passarge, J., Reijenga, C. A., Esgalhado, E., van der Weijden, C. C., Schepper, M., Walsh, M. C., Bakker, B. M., van Dam, K., Westerhoff, H. V. & Snoep, J. L. (2000) Can yeast glycolysis be understood in terms of *in vitro* kinetics of the constituent enzymes? Testing biochemistry, *Eur. J. Biochem. 267*, 5313–5329.

[80] Cronwright, G. R., Rohwer, J. M. & Prior, B. A. (2002) Metabolic control analysis of glycerol synthesis in *Saccharomyces cerevisiae*, *Appl. Environ. Microbiol. 68*, 4448–4456.

[81] Sauro, H. M. (1993) SCAMP: a general-purpose simulator and metabolic control analysis program, *Comput. Appl. Biosci. 9*, 441–450.

[82] Olivier, B., Rohwer, J. & Hofmeyr, J. (2002) Modelling cellular processes with Python and Scipy, *Mol. Biol. Rep. 29*, 249–254.

[83] Walsh, M. C., Smits, H. P., Scholte, M. & van Dam, K. (1994) The affinity of glucose transport in *Saccharomyces cerevisiae* is modulated during growth on glucose, *J. Bacteriol. 176*, 953–958.

[84] Bauchop, T. & Elsden, S. R. (1960) The growth of micro-organisms in relation to their energy supply, *J. Gen. Microbiol. 23*, 457–469.

[85] Snoep, J. L., Jensen, P. R., Groeneveld, P., Molenaar, D., Kholodenko, B. N. & Westerhoff, H. V. (1994) How to determine control of growth rate in a chemostat. Using metabolic control analysis to resolve the paradox, *Biochem. Mol. Biol. Int. 33*, 1023–1032.

[86] Weusthuis, R. A., Pronk, J. T., van den Broek, P. J. A. & van Dijken, J. P. (1994) Chemostat cultivation as a tool for studies on sugar transport in yeasts, *Microbiol. Rev. 58*, 616–630.

[87] Ferea, T. L., Botstein, D., Brown, P. O. & Rosenzweig, R. F. (1999) Systematic changes in gene expression patterns following adaptive evolution in yeast, *Proc. Natl. Acad. Sci. USA 96*, 9721–9726.

[88] Flikweert, M. T., van der Zanden, L., Janssen, W. M., Steensma, H. Y., van Dijken, J. P. & Pronk, J. T. (1996) Pyruvate decarboxylase: an indispensable enzyme for growth of *Saccharomyces cerevisiae* on glucose, *Yeast 12*, 247–257.

[89] Hofmeyr, J.-H. S. & Rohwer, J. M. (1998) Control Analysis of Adenylate-Conserving Cycles in the Absence or Presence of Adenylate Kinase, in *Bio-ThermoKinetics in the Post Genomic Era* (Larsson, C., Påhlman, I. & Gustafsson, L., eds.) pp. 7–10, Chalmers Reproservice, Göteborg.

[90] Pirt, S. J. (1975) *Principles of microbe and cell cultivation*, John Wiley and Sons, Inc, New York.

[91] Russell, J. B. & Cook, G. M. (1995) Energetics of bacterial growth: balance of anabolic and catabolic reactions, *Microbiol. Rev. 59*, 48–62.

[92] Larsson, C., von Stockar, U., Marison, I. & Gustafsson, L. (1993) Growth and metabolism of *Saccharomyces cerevisiae* in chemostat cultures under carbon, nitrogen, or carbon- and nitrogen-limiting conditions, *J. Bacteriol. 175*, 4809–4816.

[93] Lidén, G., Persson, A., Gustafsson, L. & Niklasson, C. (1995) Energetics and product formation by *Saccharomyces cerevisiae* grown in anaerobic chemostats under nitrogen limitation, *Appl. Environ. Microb. 43*, 1034–1038.

[94] Albers, E., Larsson, C., Lidén, G., Niklasson, C. & Gustafsson, L. (1996) Influence of the nitrogen source on *Saccharomyces cerevisiae* anaerobic growth and product formation, *Appl. Environ. Microbiol. 62*, 3187–3195.

[95] Visser, W., van den Baan, A. A., Batenburg-van der Vegte, W., Scheffers, W. A., Krämer, R. & van Dijken, J. P. (1994) Involvement of mitochondria in the assimilatory metabolism of anaerobic *Saccharomyces cerevisiae* cultures, *Microbiology 140*, 3039–3046.

[96] Nissen, T. L., Schulze, U., Nielsen, J. & Villadsen, J. (1997) Flux distributions in anaerobic, glucose-limited continuous cultures of *Saccharomyces cerevisiae*, *Microbiology 143*, 203–218.

[97] du Preez, J. C., de Kock, S. H., Kilian, S. G. & Litthauer, D. (2000) The relationship between transport kinetics and glucose uptake by *Saccharomyces cerevisiae* in aerobic chemostat cultures, *Anton. Leeuw. 77*, 379–388.

[98] Kroukamp, O., Rohwer, J. M., Hofmeyr, J.-H. S. & Snoep, J. L. (2002) Experimental supply-demand analysis of anaerobic yeast energy metabolism, *Mol. Biol. Rep. 29*, 203–209.

[99] Duboc, P. & von Stockar, U. (1998) Systematic errors in data evaluation due to ethanol stripping and water vaporization, *Biotechnol. Bioeng. 58*, 428–439.

[100] Koebmann, B. J., Westerhoff, H. V., Snoep, J. L., Solem, C., Pedersen, M. B., Nilsson, D., Michelsen, O. & Jensen, P. R. (2002) The extent to which ATP demand controls the glycolytic flux depends strongly on the organism and conditions for growth, *Mol. Biol. Rep. 29*, 41–45.

[101] Koebmann, B. J., Westerhoff, H. V., Snoep, J. L., Nilsson, D., & Jensen, P. R. (2002) The glycolytic flux in *Escherichia coli* is controlled by the demand for ATP, *J. Bacteriol. 184*, 3909–3916.

[102] de Atauri, P., Curto, R., Puigjaner, J., Cornish-Bowden, A. & Cascante, M. (1999) Advantages and disadvantages of aggregating fluxes into synthetic and degradative fluxes when modelling metabolic pathways, *Eur. J. Biochem. 265*, 671–679.

[103] Palsson, B. O. & Lee, I.-D. (1993) Model complexity has a significant effect on the numerical value and interpretation of metabolic sensitivity coefficients, *J. Theor. Biol. 161*, 299–315.

[104] Theobald, U., Mailinger, W., Baltes, M., Rizzi, M. & Reuss, M. (1997) In vivo analysis of metabolic dynamics in *Saccharomyces cerevisiae*: I. Experimental observations, *Biotechnol. Bioeng. 55*, 305–316.

[105] Ausubel, F. M., Brent, R., Kingston, R. E., Moore, D. D., Seidman, J. G., Smith, J. A. & Struhl, K. (eds.) (1997) *Current protocols in molecular biology*, USA, John Wiley and Sons, Inc.